



**Karolinska
Institutet**

Karolinska Institutet

<http://openarchive.ki.se>

This is a Peer Reviewed Manuscript version of the following article, accepted for publication in *Developmental cell*.

2018-02-12

Serum proteases potentiate BMP-induced cell cycle re-entry of dedifferentiating muscle cells during newt limb regeneration

Wagner, Ines; Wang, Heng; Weissert, Philipp; Straube, Werner; Shevchenko, Anna; Gentzel, Marc; Brito, Gonçalo M; Tazaki, Akira; Oliveira, Catarina; Sugiura, Takuji; Shevchenko, Andrej; Simon, András; Drechsel, David; Tanaka, Elly

Dev Cell. 2017 Mar 27;40(6):608-617.e6.

<http://doi.org/10.1016/j.devcel.2017.03.002>

<http://hdl.handle.net/10616/46223>

If not otherwise stated by the Publisher's Terms and conditions, the manuscript is deposited under the terms of the Creative Commons Attribution-NonCommercial-NoDerivatives License (<http://creativecommons.org/licenses/by-nc-nd/4.0/>), which permits non-commercial re-use, distribution, and reproduction in any medium, provided the original work is properly cited, and is not altered, transformed, or built upon in any way.



**Karolinska
Institutet**

This is an author produced version of a paper accepted by **Developmental cell**. This paper has been peer-reviewed but does not include the final publisher proof-corrections or journal pagination.

Serum proteases potentiate BMP-induced cell cycle re-entry of dedifferentiating muscle cells during newt limb regeneration

Wagner, Ines; Wang, Heng; Weissert, Philipp; Straube, Werner; Shevchenko, Anna; Gentzel, Marc; Brito, Goncalo; Tazaki, Akira; Oliveira, Catarina; Sugiura, Takuji; Shevchenko, Andrej; Simon, András; Drechsel, David; Tanaka, Elly

DOI: [10.1016/j.devcel.2017.03.002](https://doi.org/10.1016/j.devcel.2017.03.002)

Access to the published version may require subscription.
Published with permission from: **Elsevier**

Serum proteases potentiate BMP-induced cell cycle re-entry of dedifferentiating muscle cells during newt limb regeneration

Ines Wagner^{1,2,6*}, Heng Wang^{3*}, Philipp M. Weissert^{1,2,5*}, Werner L. Straube^{1,*}, , Anna Shevchenko¹, Marc Gentzel¹, Goncalo Brito³, Akira Tazaki², Catarina Oliveira^{1,2}, Takuji Sugiura², Andrej Shevchenko¹, András Simon^{3,4}, David N. Drechsel^{1,4}, Elly M. Tanaka^{2,4}

*These authors contributed equally to this work.

¹Max Planck Institute of Molecular Cell Biology and Genetics, Dresden Germany

²Technische Universität Dresden, DFG Research Center for Regenerative Therapies, Dresden Germany

³Karolinska Institute, Department of Cell and Molecular Biology, Centre of Developmental Biology for Regenerative Medicine

Current Address:

⁵European Research Institute for the Biology of Ageing, University Medical Centre Groningen, University of Groningen, Groningen, the Netherlands

⁶DKMS Life Science Lab, Fiedlerstrasse 34, Dresden, Germany

⁴Authors for correspondence and current address:

Lead contact:

Elly M. Tanaka

Institute of Molecular Pathology (IMP)

Campus Vienna Biocenter 1

1030 Vienna, AUSTRIA

Tel: + +43 1 797303200

E-mail: elly.tanaka@imp.ac.at

David N. Drechsel

Institute of Molecular Pathology (IMP)

Campus Vienna Biocenter 1

1030 Vienna, AUSTRIA

Tel: + +43 1 797303200

E-mail: david.drechsel@imp.ac.at

András Simon

Karolinska Institute, Department of Cell and Molecular Biology, Centre of Developmental Biology for Regenerative Medicine,

Berzelius väg 35

17177 Stockholm, SWEDEN

46 Email: Andras.Simon@ki.se

47

48 **Key words:** Limb Regeneration, plasmin, thrombin, BMP (Bone
49 **Morphogenetic Protein), dedifferentiation, salamander, cell cycle re-**
50 **entry**

ABSTRACT

Limb amputation in the newt induces myofibers to dedifferentiate and re-enter the cell cycle to generate proliferative myogenic precursors in the regeneration blastema. Here we show that Bone Morphogenetic Proteins (BMP) and mature BMPs that have been further cleaved by serum proteases induce cell cycle entry by dedifferentiating newt muscle cells. Protease-activated BMP4/7 heterodimers that are present in serum strongly induced myotube cell cycle re-entry with protease cleavage yielding a thirty-fold potency increase of BMP4/7 compared to canonical BMP4/7. Inhibition of BMP signaling via muscle-specific dominant-negative receptor expression reduced cell cycle entry *in vitro*, and *in vivo*. *In vivo* inhibition of serine protease activity depressed cell cycle reentry, which in turn was rescued by cleaved-mimic BMP. This work identifies a mechanism of BMP activation that generates blastema cells from differentiated muscle.

INTRODUCTION

In several regeneration contexts, cells of mature phenotype re-enter the cell cycle to help regenerate missing structures. After lentectomy in the newt, dorsal iris pigmented epithelial cells (PEC) lose pigmentation, re-enter the cell cycle and transdifferentiate to regenerate the lens (Okada, 1991) (Grogg et al., 2005). During heart regeneration, cardiac myocytes re-enter the cell cycle and apparently expand to replace injured tissue (Jopling et al., 2010; Kikuchi et al., 2010). During newt limb regeneration, skeletal muscle fibers dedifferentiate by cellularization of syncytial muscle fibers, down-regulation of muscle-specific proteins, and re-entry into the cell cycle to generate proliferative blastema cells, a process involving cell death-related pathways (Sandoval-Guzman et al., 2014) (Wang et al., 2015). The molecular pathways that initiate proliferation of dedifferentiating skeletal muscle and how the signal is activated by limb amputation remains poorly characterized. Recent findings have identified a MARCKS (Myristoylated alanine-rich C-kinase substrate)-like protein as an epithelially-expressed factor that stimulates proliferation of both resident stem cells as well as of dedifferentiated myofibre progeny (Sugiura et al., 2016). Given that the repression of many of the canonical signalling pathways inhibits regeneration, the possibility that injury-activation of a canonical pathway was also involved lay open (Beck et al., 2001; Lin and Slack, 2008) (Poss, 2010).

The local activities of serum proteases that regulate blood clotting are associated with initiation of regeneration. Regenerating newt limbs show localization of thrombin proteolytic activity (Tanaka et al., 1999) and inhibition of thrombin

activity repressed iris PEC proliferation (Imokawa and Brockes, 2003) (Godwin et al., 2010). *In vitro*, newt skeletal myotubes re-entered cell cycle after exposure to serum, an effect that was strongly potentiated by thrombin and plasmin treatment (Tanaka et al., 1999; Tanaka et al., 1997). These results implied that circulating plasma contains a cell cycle inducing activity that is highly activated by proteolytic cleavage. Biochemical characterization and partial purification of the activity indicated that it is a high molecular weight glycoprotein with defined chromatographic properties (Straube et al, 2004).

An important goal motivated by these results has been to identify the substrates of clotting proteases that induce cell cycle re-entry during regeneration. Is there a growth stimulatory factor that is a direct protease target, or do serum proteases act indirectly by cleaving an inhibitor? Here by assaying newt skeletal myotube cell cycle re-entry we show that BMP4-containing heterodimers as the major serum component required and sufficient for myotube cell cycle re-entry. We further show that BMPs have at least two major cleavage sites that are differentially sensitive to thrombin and plasmin. The combined cleavage results in up to thirty-fold potency increase of BMP4/7. *In vivo* blockage of BMP signaling specifically in dedifferentiating muscle fibers negatively affects S-phase entry. Furthermore, the *in vivo* inhibition of serum protease activity depresses the BMP-dependent S-phase entry that is in turn rescued by a cleaved-mimic BMP. An additional, and in a broader context, significant conclusion of our quantitative studies is that the detection of serum BMP4 has previously been underestimated by up to 1000-fold due to unrecognized lack of the N-terminal epitopes of serum BMPs used for ELISA quantification.

120

121 **RESULTS**

122 **Potent forms of BMP4-containing dimers in serum stimulate newt myotube**

123 **S-phase re-entry**

124 The application of fractionated serum samples to cultured newt myotubes
125 results in their concentration-dependent re-entry into S-phase, quantitated as
126 the percentage of myotubes incorporating BrdU during a 12 hours pulse (Tanaka
127 et al., 1997). We used this quantitative myotube response to measure the amount
128 of “S-phase Re-entry inducing Factor” (SPRF), in different fractions from serum.
129 By quantitating activity versus total protein concentration we had previously
130 found that SPRF activity is enriched by 20-fold over serum in commercially
131 produced, low-purity bovine thrombin preparations and that it was possible to
132 separate SPRF from its activator using several different chromatographic
133 methods (Tanaka et al., 1999)(Straube et al, 2004). To molecularly identify SPRF,
134 the thrombin preparation was subjected to four sequential steps of column
135 chromatography (Figure S1A). The specific activity of SPRF was measured
136 across sequential fractions from each column and fractions containing the peak
137 of activity were pooled and applied to the next chromatography step. “Fold
138 purification” was calculated based on the fold increase in specific activity found
139 in the peak pool and “yield” was calculated based on the total amount of activity
140 found in the peak pool from each step (Figure S1A). The most purified fraction
141 was subjected to non-reducing SDS-PAGE. Mass spectrometry analysis of trypsin-
142 digested proteins of the gel regions between 28-39 kD identified 34 major
143 proteins that included BMP4, BMP5, and BMP7 (Table S3). A visual screen of 16
144 commercially available recombinant proteins on the myotube assay suggested

that only BMP4 could induce a myotube response. To determine if the presence of BMP4 correlated with the increased purification of SPRF, we performed western blotting after loading equal amounts of total protein from the peak pools on SDS PAGE. The starting material and peak pool from the cation exchange step showed undetectable levels of BMP4 whereas we observed a highly enriched representation of BMP4 in the last two column steps (Figure S1B). Western blotting across the last size exclusion fractionation (equal volume loading of samples) showed correlation between the BMP4 signal and the S-phase re-entry activity (Figure S1D). BMP5, BMP6 and BMP7 were not detectable using currently available ELISA and western blot reagents, BMP2 which is in the same subfamily as BMP4 and very similar in sequence was detected in the most purified fractions although it had not been detected by MS (Figure S1C). These results indicated that the presence of BMP4 and possibly BMP2 correlated quantitatively with the presence of SPRF activity during the purification.

To determine if BMP4 accounts for at least part of the SPRF activity, we assayed recombinant bovine BMP4 homodimers (bBMP4/4) on newt myotubes but surprisingly high concentrations were required to elicit a response. Recombinant bBMP4/4 and bBMP7/7, individually or in combination stimulated 50% maximal S-phase response at 47 to 77 ng/ml (1.9 to 3.0 nM) (Figure 1A). In contrast the native bBMP4 present in the SPRF purification fractions induced 50% maximal S-phase response at an apparent concentration of 0.06 ng/ml (2.4 pM) (Figure 1A). These results suggested that either native BMP4 containing dimers were intrinsically more potent than recombinantly produced proteins, or accessory factors work in parallel to or in concert with native BMPs to account for their

increased potency. To investigate this discrepancy we first assayed recombinant bBMP4/7 heterodimers. Consistent with previous reports (Israel et al., 1996) that BMP heterodimers have higher activity than homodimers, the recombinant bBMP4/7 heterodimer showed approximately 19-fold higher potency when compared with recombinant bBMP4/4 homodimer (Figure 1A, Figure S2A) but this still left a 40-fold discrepancy in activity between native BMPs in the purified SPRF material and the recombinant BMP preparations.

To determine if BMPs represent a major part of the activity in the serum preparations, we added recombinant noggin-FC, a stoichiometric, pan-specific inhibitor of BMPs (Holley et al., 1996; Zimmerman et al., 1996), to both partially purified SPRF and to recombinant bBMP preparations, and found extinction of activity (Figure 1B). Noggin-Fc also inhibited the cell cycle re-entry activity present in fetal calf serum (Figure S2B). Using noggin-FC as an affinity reagent, we specifically depleted BMPs from a partially purified SPRF preparation and found depletion of activity that could be quantitatively recovered using 1% SDS as eluate (Figure 1C). The eluate was separated on non-reducing SDS-PAGE, proteins were retrieved from gel slices and recovery of bioactivity found in the size range of 28-36 kD in this eluate (Figure 1D). Mass spectrometry analysis of this gel slice identified BMP2, BMP4, BMP5, BMP6 and BMP7.

We then specifically immunodepleted BMP4 from the Butyl20 fraction using polyclonal antibodies and correspondingly observed a loss of activity which could be quantitatively recovered from the immunoprecipitate (Figure 1E). This result shows that BMP4-containing homo- or heterodimers are a major and

sufficient constituent of the activity. Mass spectrometry analysis of the active region of a non-reducing gel between 28 and 36 kD identified BMP2, BMP4, BMP5, BMP6 and BMP7 (Table S1). Since no detectable cross-reaction of the anti-BMP4 antibody was observed with BMP5, BMP6 and BMP7 these results strongly suggest that the serum preparations contain BMP2/4, BMP4/5, BMP4/6 and BMP4/7 heterodimers. Taken together these results show that BMP-containing dimers account for the SPRF activity and are sufficient for cell cycle re-entry in newt myotubes.

Activated BMPs are cleaved at multiple target sites by thrombin and plasmin

Considering the large discrepancy in potency between serum-derived BMPs versus recombinant BMP4/7, and earlier observations that the serum factor is activated by thrombin and plasmin proteolysis, we investigated whether BMPs are direct targets of thrombin and plasmin. The treatment of recombinant hBMP4/7 with purified thrombin resulted in a 10-15-fold increase in activity while treatment with plasmin resulted in a 20-30-fold increase in activity (Figure 2A). Plasmin and thrombin also induced increased potencies in the recombinant hBMP2/2, hBMP4/4 and hBMP7/7 (Figure 2B, Figure S2C-D). We noticed in western blots reduced signal for protease treated BMP2, BMP4 and BMP7 (Figure 2C) which could have reflected either a general proteolytic degradation of proteins or an alteration of a major epitope for antibody binding. We therefore analyzed purified, bacterially-produced recombinant hBMP4/4 after plasmin or thrombin treatment by silver staining versus western blot. Human BMPs were the only available preparations with sufficient purity for such

220 detailed biochemical analysis and are practically identical in sequence to bovine
221 BMP4 (1 amino acid substitution) so we performed the analyses in Figure 2 and
222 subsequent work with human recombinant BMPs. Silver staining showed a
223 progressive appearance of multiple lower molecular weight bands with
224 increased incubation with plasmin and thrombin, but the overall protein level
225 remained constant, excluding generalized proteolytic degradation, but rather
226 suggesting that an alteration of the epitope responsible for antibody binding
227 (Figure 2D).

228

229 We next pursued mapping the target sites on BMP4 for thrombin and plasmin.
230 Thrombin cleaves the peptide bond following positively charged residues with
231 high selectivity while plasmin cleaves the peptide bond following lysine or
232 arginine residues with relatively relaxed surrounding sequence requirements
233 (Mattler and Bang, 1977; Ryan et al., 1976; Vindigni, 1999). The BMP4 N-
234 terminus contains multiple lysine and arginine residues, which when cleaved
235 would cause the N-terminus to be cleaved into small fragments and released
236 (Figure S3). This N-terminal domain has previously been characterized as a
237 heparin-binding domain that causes BMP retention in heparin-containing gels
238 and can be removed by plasmin treatment, which results in higher BMP2
239 bioactivity on alkaline phosphatase induction assay (Ruppert et al., 1996; Uludag
240 et al., 2001) (Roedel et al., 2013). In addition BMP4 also contains lysine residues
241 in the centrally (K78) and in the C-terminus (K99, K103) with the K103 site
242 representing an ideal plasmin substrate sequence, conserved among BMPs. Due
243 to intramolecular disulfide bonding, the peptides resulting from such cleavages

244 are predicted to remain covalently associated with the mature dimer (Figure
245 S3E).

246

247 To map the thrombin and plasmin-associated cleavage sites we employed
248 Edman sequencing of hBMP4/4 and hBMP4/7, which detects newly generated N-
249 terminal amino acids after protein cleavage. We first analyzed hBMP4/4 to
250 understand cleavage sites on the BMP4 polypeptide alone. The untreated sample
251 yielded the sole presence of the classical N-terminus of the mature BMP4, SPKHH
252 (Figure S3A, pink, Data S1, Table S2). Thrombin treated BMP4/4 revealed a
253 single new N-terminus -ARKKNK- as (Figure S3A, green, Data S1, Table S2)
254 indicating that thrombin targets arginine (R8) which is also consistent with gel
255 mobility data (Figure 2D, Figure S3B). In contrast, plasmin-treated BMP4/4
256 yielded two N-termini, KKNKN, and NYQEM indicating that plasmin targets R10
257 and K103 (Figure S3A, orange, Data S1, Table S2) consistent with gel mobility
258 data showing the appearance of two major lower molecular weight peptides
259 (Figure S3B). These findings suggest that the increased potency of plasmin-
260 treated BMPs derives from the additional cleavage at K103 (Figure S3A , Data S1,
261 Table S2).

262

263 To confirm the C-terminal plasmin site, we also performed mass spectrometry
264 and compared the presence of peptides in preparations that had or had not been
265 reduced and alkylated (to break disulfide bridges and prevent their re-
266 formation). The C-terminal peptides NYQEMVVEGCGCR and some traces of
267 VVLKNYQEMVVEGCGCR were the major peptides detected in the plasmin-
268 treated samples that had been reduced and alkylated but were not present in the

non-reduced samples. This result confirms the occurrence of plasmin-mediated cleavage at the C-terminal K99 and/or K103 residues and retention in the native dimer via disulfide bonds.

Since we had observed a high shift in potency of plasmin-cleaved BMP4/7 (Figure 2A, Figure S3C), we performed Edman sequencing of the plasmin derived non-reduced recombinant human BMP4/7 to determine cleavage sites in BMP7. The analysis yielded the BMP4 sequences -NYQEM- and -KKNKN as well as three BMP7 sequences, DLGWQDW, MANVAEN, NMVVRAC, indicating cleavage of BMP7 in several internal locations (Figure S3A, Data S1, Table S2). These results show that BMP4 and BMP7 have plasmin cleavage sites beyond the previously known N-terminal K8 sequence on BMP2 (Roedel et al., 2013; Uludag et al., 2001). Cleavage at these sites maintains an intact BMP molecule in the disulfide bonded state, and correlates with the increased ability of plasmin to activate the BMP4/7 heterodimer.

***In vivo* cell cycle entry of dedifferentiating muscle involves SMAD-mediated BMP signaling and is protease-sensitive**

To test the role of BMP signaling in S-phase entry of skeletal muscle cells *in vivo*, we sought to autonomously block BMP signaling in newt skeletal muscle fibers by expression of dominant negative BMP receptors (dnBMPR). To validate the dnBMPRs, we first transfected myotubes *in vitro* with *dnAlkL2*, *dnAlkL3* and *dnAlkL6* expression constructs together with a *nucGfpFP* construct and then challenged them 24 hours after plating with recombinant hBMP4/7. In control samples transfected with *nucGfpFP* only, S-phase response in GFP⁺ myotubes

Formatted: Font: Italic

Formatted: Font: Italic

Formatted: Font: Italic

Formatted: Font: Italic

Formatted: Font: Italic

was 24±4%. In contrast all tested dnBMPR including *dnAlk~~2~~2*, *dnAlk3* and *dnAlk~~3~~6* yielded strong suppression of the S-phase response to 2.0 ± 1.8% (p = 2.26 x 10⁻⁰⁸), 6.5 ± 4.6% (p = 7.12 x 10⁻⁰⁹) and 0.2 ± 0.6% (p = 7.47 x 10⁻⁰⁸) respectively (Figure 3A). These results indicate that blockage of BMP signaling within the myotube is sufficient to block the S-phase response.

To block signaling *in vivo*, we specifically expressed DNA constructs in newt skeletal muscle fibers via the co-electroporation of a muscle-specific *MCK:cre*, a loxP expression cassette *CAGGs: loxP-Cherry 3PA-loxP-Histone2B-YFP* or *CAGGs: loxP-Cherry 3PA-loxP-Histone2B-YFP-T2A-dnALK* flanked by Tol2 transposon sites, and a Tol2 transposase expression plasmid (Sandoval-Guzman et al., 2014). This procedure yields expression of the H2B-YFP and dnALKs specifically in MHC⁺ muscle fibers of the intact limb. Upon limb amputation, muscle fibers cellularize prior to S-phase entry yielding YFP⁺/MHC⁻ proliferating cells in the regeneration blastema as assessed by PCNA staining and by incorporation of nucleotide analogues (Sandoval-Guzman et al., 2014). To assay DNA synthesis in cells deriving from labeled fibers, electroporated limbs were injected daily with EdU 8-13 days post-limb amputation prior to harvesting (Figure 3B). In control limbs expressing H2B-YFP alone, 67.2±6.8% of muscle derived YFP⁺MHC⁻ cells in the blastema had incorporated EdU (Figure 3C-E). In contrast, expression of dnALK2, dnALK3 or dnALK6 with H2B-YFP yielded a lower EdU labeling index of 47 ± 7.6% (p = 0.1106), 41 ± 8.4%(p = 0.0522), 43.2 ± 6.2% (p = 0.042), respectively, indicating the participation of BMP signaling during S-phase of skeletal muscle derived cells (Figure 3E). These results indicated that BMP

318 signaling is acting to promote cell cycle re-entry *in vivo* in dedifferentiating
319 muscle cells.

320

321 To determine whether the BMP signaling proceeded via intracellular SMAD
322 activity we used a SMAD-luciferase reporter (Collery and Link, 2011;
323 Korchynskyi and ten Dijke, 2002). Cultured newt myotubes transfected with the
324 reporter displayed a BMP4/7-dependent induction of luciferase activity. This
325 response was blocked by provision of the BMP-inhibitor, noggin, indicating that
326 the newt myotube response to BMP activates SMAD signaling (Figure 4A).

327 Transfection of this reporter *in vivo* into the limb blastema also showed
328 increased reporter activity during the stage of muscle dedifferentiation, at 6 and
329 12 days post-amputation (Figure 4B). The limb blastema consists of cells
330 deriving from different tissues. To directly determine if SMAD signaling takes
331 place in dedifferentiating muscle cells, we labeled muscle fibers with H2B-YFP
332 via electroporation as described above and performed immunofluorescence
333 staining for nuclear pSMAD1/5/8 staining. As shown in Figure 4C, YFP⁺ cells
334 showed nuclear pSMAD1/5/8 staining confirming the implementation of SMAD
335 activity during muscle dedifferentiation.

336

337 We next aimed to examine the relevance of BMP protease activation to *in vivo*
338 muscle cell cycle re-entry. We first assessed *in vitro* the relative effectiveness of
339 recombinantly produced WT BMP to a mutant BMP lacking the N-terminus (Δ N-
340 BMP4) that mimics the N-terminally cleaved form by assaying identically
341 produced proteins in the linear range on myotubes. Volume for volume the Δ N-
342 BMP4 more potently induced cell cycle re-entry than the full-length protein

(Figure 4D). Mutations in the C-terminal site prevented efficient production of secreted BMP and therefore, this C-terminal cleavage could not be analysed by mutational analysis (data not shown).

We then compared the *in vivo* effectiveness of the WT and Δ N forms to accelerate dedifferentiating myofiber cell cycle entry by overexpressing the BMPs in the early blastema and then assaying the proliferation of muscle cell progeny by MCM2 staining at 13 dpa. Injection of equal amounts of baculovirus for the two constructs showed a higher proliferation index of dedifferentiating muscle-derived cells in samples expressing Δ N-BMP4 compared to the full length BMP4 (Figure 4F,G). Finally we asked if inhibition of serine proteases in the amputated limb reduced cell cycle entry of muscle-derived cells upstream of BMP. Injection of YFP-muscle-labeled limbs with AEBSF, an irreversible inhibitor of both thrombin and plasmin (Powers et al., 2002), depressed EdU incorporation in YFP⁺ muscle fiber-derived cells compared to PBS-injected limbs (Figure S4A,B). Expression of the Δ N-BMP4 restored EdU incorporation in YFP⁺ muscle fiber-derived cells showing that serine protease activity acts upstream of cleaved-BMP-dependent muscle cell cycle re-entry (Figure S4C). This epistasis analysis confirms a role for protease activity as a positive, upstream regulator of BMP-driven induction of the cell cycle during limb regeneration.

DISCUSSION

Here we identify BMPs as serum factors that can stimulate cell cycle entry of differentiated newt skeletal myotubes and muscle fibers, a key step in muscle dedifferentiation during limb regeneration. We further show that BMP activity is

368 potentiated by cleavage mediated by thrombin and plasmin. These observations
369 lead to a model in which resting skeletal muscle fibers in the intact limb remain
370 sequestered from plasma BMPs that are circulating within intact blood vessels.
371 Limb amputation damages the endothelium that leaks plasma BMPs into
372 surrounding tissues and initiates the clotting cascade triggering not only fibrin
373 clot formation, but also proteolytic processing of BMPs. The progeny of the
374 damaged muscle fibers are exposed to and respond to these activated BMPs with
375 cell cycle re-entry.

376
377 The expression of BMP4 is also upregulated early after limb amputation in
378 Xenopus and Axolotl which would also be a target of activating proteolysis,
379 further reinforcing BMP action during early regeneration (Beck et al., 2006;
380 Guimond et al., 2010; Knapp et al., 2013) (Kochegarov et al., 2015). Another
381 potential BMP source is peripheral nerves, as BMP2 and BMP7 were shown to
382 substitute a proregenerative role of nerves in the accessory limb model and are
383 expressed in DRG neurons (Makanae et al., 2014). Two inhibition studies
384 implicated BMP signaling in early steps of limb regeneration, but since inhibition
385 of the pathway had been elicited by global expression of noggin, it was unclear if
386 the negative effects on cell proliferation had been through a direct or indirect
387 means (Beck et al., 2006; Guimond et al., 2010; Knapp et al., 2013). Here, through
388 cell autonomous inhibition of BMP signaling, we show a direct effect of the
389 pathway on muscle-derived cell cycle entry. This pathway appears to be
390 working in parallel to the recently described MLP pathway (Sugiura et al., 2016)
391 which would explain the partial loss of EdU incorporation when we blocked BMP
392 signaling in in vivo muscle fibers, while we observed complete block of S-phase

393 in response to serum in the *in vitro* assay system, where MLP was not present in
394 the culture.

395

396 In other biological systems, recombinant BMP4/4 had been used to implicate
397 BMP4/4 as a potential bioactive serum factor that could support mouse ES cell
398 pluripotency and the conversion of oligodendrocyte precursors into a neural
399 stem-like cell, but a paradox existed in which the concentrations of recombinant
400 BMPs required for cell stimulation did not match the very low concentrations of
401 BMPs measured in serum (Kondo and Raff, 2000; Ying et al., 2003) (Park et al.,
402 2008; Tacke et al., 2007; Wendling et al., 2007). Therefore it was unclear
403 whether other serum factors were really required. Our biochemical approach
404 provides an explanation that could resolve this controversy. First we show that
405 in our *in vitro* assay, serum BMPs quantitatively account for the activity. Our
406 work also strongly suggests that a significant fraction of the BMP4 in serum is
407 complexed to BMP5, 6 and 7 as heterodimers. This is important considering that
408 BMP4/7 is more potent than BMP4/4 in our and other cellular assays. Next our
409 work indicates that the quantification of serum BMPs by western blot or ELISA
410 vastly underestimates the concentration of BMPs in serum. ELISAs used to
411 quantitate BMP4 and BMP7 employ antibodies that are directed against the N-
412 terminus. Our work shows that since the N-terminus is lacking in serum BMPs,
413 the vast majority of BMPs present in serum are likely not detected. Using ELISA
414 kits, the serum concentration of BMP4 has been estimated at 0.04 ng/ml and
415 BMP7 at 0.01-0.28 ng/ml (Park et al., 2008; Tacke et al., 2007; Wendling et al.,
416 2007). Based on our measurements of the loss of immunoreactivity in western
417 blots using a commercial polyclonal anti-BMP antibody, and the enrichment of

BMP activity along the different steps of purification, we calculate that BMP4 is present in serum at a concentration of 20-100 ng/ml, which is 1000-fold higher than previous estimations. Significantly, the re-estimated concentration of this molecule is at levels highly relevant to cellular assays.

In summary, our work provides insight into how a local injury initiates activation of the BMP signaling pathway and how this signaling pathway acts directly on a cellular mechanism involved in generating blastema cells from mature tissue, namely cell cycle entry during dedifferentiation of muscle fibers. This molecular insight has important implications for promoting a proliferative state for the purpose of regeneration.

EXPERIMENTAL PROCEDURES

See STAR methods page.

ACKNOWLEDGEMENTS: This work was supported by BMBF Biofutures (EMT), MPI-CBG (EMT, DND, ASh) and the CRTD (EMT) and by the Swedish Research Council, Wenner-Gren Foundation and Cancerfonden to ASi. We thank Walter Sebald for bacterially expressed human BMP2/2 and BMP4/4, and Barbara Borgonova, Mike Tipsword, Regis Lemaitre and Elena Taverna for technical assistance and Michael Kiess (Toplab GmbH) for Edman sequencing.

AUTHOR CONTRIBUTIONS: IW, PW, WLS, AT, ~~MG, ASh~~, TS, DND performed and analyzed in vitro BMP characterization and myotube assays. [MG, Anna Shev.](#), [Andrei Shev. performed mass spectrometry analysis.](#) HW, GC, ~~CO~~ performed in

443 | vivo [newt](#) experiments. [CO made baculovirus for in vivo experiments](#) IW, HW,
444 | A[Simon](#), EMT analysed data and wrote the manuscript.

References

- Beck, C.W., Christen, B., Barker, D., and Slack, J.M. (2006). Temporal requirement for bone morphogenetic proteins in regeneration of the tail and limb of *Xenopus* tadpoles. *Mech Dev* 123, 674-688.
- Beck, C.W., Whitman, M., and Slack, J.M. (2001). The role of BMP signaling in outgrowth and patterning of the *Xenopus* tail bud. *Dev Biol* 238, 303-314.
- Collery, R.F., and Link, B.A. (2011). Dynamic smad-mediated BMP signaling revealed through transgenic zebrafish. *Dev Dyn* 240, 712-722.
- Ferretti P, Brockes JP. (1988). Culture of newt cells from different tissues and their expression of a regeneration-associated antigen. *J Exp Zool.* 247, 77-91.
- Godwin, J.W., Liem, K.F., Jr., and Brockes, J.P. (2010). Tissue factor expression in newt iris coincides with thrombin activation and lens regeneration. *Mech Dev* 127, 321-328.
- Grogg, M.W., Call, M.K., Okamoto, M., Vergara, M.N., Del Rio-Tsonis, K., and Tsonis, P.A. (2005). BMP inhibition-driven regulation of six-3 underlies induction of newt lens regeneration. *Nature* 438, 858-862.
- Guimond, J.C., Levesque, M., Michaud, P.L., Berdugo, J., Finnson, K., Philip, A., and Roy, S. (2010). BMP-2 functions independently of SHH signaling and triggers cell condensation and apoptosis in regenerating axolotl limbs. *BMC Dev Biol* 10, 15.
- Holley, S.A., Neul, J.L., Attisano, L., Wrana, J.L., Sasai, Y., O'Connor, M.B., De Robertis, E.M., and Ferguson, E.L. (1996). The *Xenopus* dorsalizing factor noggin ventralizes *Drosophila* embryos by preventing DPP from activating its receptor. *Cell* 86, 607-617.
- Imokawa, Y., and Brockes, J.P. (2003). Selective activation of thrombin is a critical determinant for vertebrate lens regeneration. *Curr Biol* 13, 877-881.
- Israel, D.I., Nove, J., Kerns, K.M., Kaufman, R.J., Rosen, V., Cox, K.A., and Wozney, J.M. (1996). Heterodimeric bone morphogenetic proteins show enhanced activity in vitro and in vivo. *Growth Factors* 13, 291-300.
- Jopling, C., Sleep, E., Raya, M., Marti, M., Raya, A., and Belmonte, J.C. (2010). Zebrafish heart regeneration occurs by cardiomyocyte dedifferentiation and proliferation. *Nature* 464, 606-609.
- Kikuchi, K., Holdway, J.E., Werdich, A.A., Anderson, R.M., Fang, Y., Egnaczyk, G.F., Evans, T., Macrae, C.A., Stainier, D.Y., and Poss, K.D. (2010). Primary contribution to zebrafish heart regeneration by gata4(+) cardiomyocytes. *Nature* 464, 601-605.
- Knapp, D., Schulz, H., Rascon, C.A., Volkmer, M., Scholz, J., Nacu, E., Le, M., Novozhilov, S., Tazaki, A., Protze, S., et al. (2013). Comparative transcriptional profiling of the axolotl limb identifies a tripartite regeneration-specific gene program. *PLoS One* 8, e61352.
- Kochegarov, A., Moses-Arms, A., M.C., H., and Lemanski, L.F. (2015). Identification of Genes Involved in Limb Regeneration in the Axolotl *Ambystoma mexicanum*. *JSM Regenerative Medicine & Bioengineering* 3.
- Kondo, T., and Raff, M. (2000). Oligodendrocyte precursor cells reprogrammed to become multipotential CNS stem cells. *Science* 289, 1754-1757.
- Korchynskyi, O., and ten Dijke, P. (2002). Identification and functional characterization of distinct critically important bone morphogenetic protein-specific response elements in the Id1 promoter. *J Biol Chem* 277, 4883-4891.

492 Lin, G., and Slack, J.M. (2008). Requirement for Wnt and FGF signaling in *Xenopus*
 493 tadpole tail regeneration. *Dev Biol* 316, 323-335.
 494 Liu F, Ventura F, Doody J, Massague J.(1995). Human type II receptor for bone
 495 morphogenic proteins (BMPs): extension of the two-kinase receptor model to
 496 the BMPs. *Mol Cell Biol* 7, 3479-86
 497 Magaud JP, Sargent I, Mason DY. (1988). Detection of human white cell
 498 proliferative responses by immunoenzymatic measurement of
 499 bromodeoxyuridine uptake. *J Immunol Methods*. 106, 95-100.
 500 Makanae, A., Mitogawa, K., and Satoh, A. (2014). Co-operative Bmp- and Fgf-
 501 signaling inputs convert skin wound healing to limb formation in urodele
 502 amphibians. *Dev Biol* 396, 57-66.
 503 Mattler, L.E., and Bang, N.U. (1977). Serine protease specificity for peptide
 504 chromogenic substrates. *Thromb Haemost* 38, 776-792.
 505 Nacu E, Gromberg E, Oliveira CR, Drechsel D, Tanaka EM. (2016). FGF8 and SHH
 506 substitute for anterior-posterior tissue interactions to induce limb regeneration.
 507 *Nature*. 533, 407-10.
 508 Okada, T.S. (1991). *Transdifferentiation : flexibility in cell differentiation*. (Oxford
 509 Oxford ; New York: Clarendon Press ;
 510 Oxford University Press).
 511 Park, M.C., Park, Y.B., and Lee, S.K. (2008). Relationship of bone morphogenetic
 512 proteins to disease activity and radiographic damage in patients with ankylosing
 513 spondylitis. *Scand J Rheumatol* 37, 200-204.
 514 Poss, K.D. (2010). Advances in understanding tissue regenerative capacity and
 515 mechanisms in animals. *Nat Rev Genet* 11, 710-722.
 516 Powers, J.C., Asgian, J.L., Ekici, O.D., and James, K.E. (2002). Irreversible inhibitors
 517 of serine, cysteine, and threonine proteases. *Chemical reviews* 102, 4639-4750.
 518 Roedel, E.K., Schwarz, E., and Kanse, S.M. (2013). The factor VII-activating
 519 protease (FSAP) enhances the activity of bone morphogenetic protein-2 (BMP-2).
 520 *J Biol Chem* 288, 7193-7203.
 521 Ruppert, R., Hoffmann, E., and Sebald, W. (1996). Human bone morphogenetic
 522 protein 2 contains a heparin-binding site which modifies its biological activity.
 523 *Eur J Biochem* 237, 295-302.
 524 Ryan, T.J., Fenton, J.W., 2nd, Chang, T., and Feinman, R.D. (1976). Specificity of
 525 thrombin: evidence for selectivity in acylation rather than binding for p-
 526 nitrophenyl alpha-amino-p-toluate. *Biochemistry* 15, 1337-1341.
 527 Sandoval-Guzman, T., Wang, H., Khattak, S., Schuez, M., Roensch, K., Nacu, E.,
 528 Tazaki, A., Joven, A., Tanaka, E.M., and Simon, A. (2014). Fundamental Differences
 529 in Dedifferentiation and Stem Cell Recruitment during Skeletal Muscle
 530 Regeneration in Two Salamander Species. *Cell Stem Cell* 14, 174-187.
 531 Straube, W.L. Brockes, J.P., Drechsel, D.N., Tanaka, E.M. (2004). Plasticity and
 532 reprogramming of differentiated cells in amphibian regeneration: partial
 533 purification of the serum factor that triggers cell cycle re-entry in differentiated
 534 muscle cells. *Cloning and Stem Cells* 6, 333-344
 535 Sugiura, T., Wang, H., Barsacchi, R., Simon, A., and Tanaka, E.M. (2016). MARCKS-
 536 like protein is an initiating molecule in axolotl appendage regeneration. *Nature*
 537 531, 237-240.
 538 Tacke, F., Gabele, E., Bataille, F., Schwabe, R.F., Hellerbrand, C., Klebl, F., Straub,
 539 R.H., Luedde, T., Manns, M.P., Trautwein, C., et al. (2007). Bone morphogenetic

protein 7 is elevated in patients with chronic liver disease and exerts fibrogenic effects on human hepatic stellate cells. *Dig Dis Sci* 52, 3404-3415.

Tanaka, E.M., Drechsel, D.N., and Brockes, J.P. (1999). Thrombin regulates S-phase re-entry by cultured newt myotubes. *Curr Biol* 9, 792-799.

Tanaka, E.M., Gann, A.A., Gates, P.B., and Brockes, J.P. (1997). Newt myotubes reenter the cell cycle by phosphorylation of the retinoblastoma protein. *J Cell Biol* 136, 155-165.

Uludag, H., Gao, T., Porter, T.J., Friess, W., and Wozney, J.M. (2001). Delivery systems for BMPs: factors contributing to protein retention at an application site. *The Journal of bone and joint surgery. American volume* 83-A *Suppl 1*, S128-135.

Vindigni, A. (1999). Energetic dissection of specificity in serine proteases. *Comb Chem High Throughput Screen* 2, 139-153.

Wang, H., Loof, S., Borg, P., Nader, G.A., Blau, H.M., and Simon, A. (2015). Turning terminally differentiated skeletal muscle cells into regenerative progenitors. *Nature communications* 6, 7916.

Webster C, Silberstein L, Hays AP, Blau HM. (1988). Fast muscle fibers are preferentially affected in Duchenne muscular dystrophy. *Cell*. 52, 503-13.

Wendling, D., Cedoz, J.P., Racadot, E., and Dumoulin, G. (2007). Serum IL-17, BMP-7, and bone turnover markers in patients with ankylosing spondylitis. *Joint Bone Spine* 74, 304-305.

Ying, Q.L., Nichols, J., Chambers, I., and Smith, A. (2003). BMP induction of Id proteins suppresses differentiation and sustains embryonic stem cell self-renewal in collaboration with STAT3. *Cell* 115, 281-292.

Zimmerman, L.B., De Jesus-Escobar, J.M., and Harland, R.M. (1996). The Spemann organizer signal noggin binds and inactivates bone morphogenetic protein 4. *Cell* 86, 599-606.

Zou H, Wieder R, Massague J, Niswander L. (1997). Distinct roles of type I bone morphogenetic protein receptors in the formation and differentiation of cartilage. *Genes Dev*. 11, 2191-2203

FIGURE LEGENDS

Fig. 1. BMP4 containing dimers are necessary and sufficient for S-phase re-entry, but recombinant molecules are less potent than native BMP4s.

(A) Dose response curves for recombinant bovine BMP4/4, BMP7/7 and BMP4/7. Square, green: Serum-derived BMP4 (SPRF); diamond, pink: recombinant BMP4/7; triangle, blue: recBMP4/4; inverted triangle, red: recBMP7/7; circle, lilac: mixture of recBMP4/4 plus recBMP7/7. Data are presented as mean \pm SEM (n = 3).

(B) Addition of Noggin-FC to BMPs or SPRF inhibits S-phase. Square, green: Serum-derived BMP4 (SPRF); circle, pink: recombinant BMP4/7 heterodimer. Data are presented as mean \pm SEM (n = 3).

(C) Noggin-FC-mediated depletion of BMPs and recovery from eluate. SPRF was pre-incubated with ProteinG beads (SPRF, PrG bead dep.) then incubated with noggin-FC-linked beads (SPRF, noggin-FC + PrG bead dep.). Elution from bound beads in 1% SDS (noggin-FC eluate) results in recovery of activity. Data are presented as mean \pm SEM (n = 9). Significance calculated by Student's t-test.

(D) Sample eluted from the noggin-FC precipitate using 1% SDS (noggin-FC eluate) was separated on non-reducing SDS-PAGE and protein recovered by electroelution from gel slices as indicated. Positive activity in bioassay is observed in the gel slice in the size range of 28-36 kD (gel slice 7). Data are presented as mean \pm SEM (n = 3).

(E) Immunodepletion of BMP4 from serum fraction depletes activity and elution recovers activity. SPRF was first pre-incubated with ProteinG beads (SPRF, PrG bead dep.) then incubated with anti-BMP4 antibody-linked beads for immunodepletion (SPRF, α BMP4 + PrG bead dep.). Elution from bound beads at pH11.5 (α BMP4 eluate) results in recovery of activity. Data are presented as mean \pm SEM (n = 9) (SPRF, PrG bead dep. and SPRF, α BMP4 + PrG bead dep.) and n = 54 (α BMP4 eluate)). (see also Table S1)

Fig. 2. Increased potency of recombinant BMP4/7 after thrombin and plasmin treatment.

(A) Dose response of untreated recombinant human BMP4/7 (circle, green, solid line) and after treatment with thrombin (inverted triangle, blue, dotted line) or plasmin (square, red, dashed line). Data are presented as mean \pm SEM (n = 3).

(B) Plasmin enhances the potency of human BMPs. Recombinant hBMP2/2 (circle, green line), BMP4/4 (square, purple line) or BMP7/7 (triangle, pink line) were incubated with increasing levels of plasmin. Samples were assayed on newt myotubes. Data are presented as mean \pm SEM (n = 3).

(C) Western blot analysis of hBMP samples before and after plasmin treatment. Lanes 1-4: rhBMP2: 0.48 ng, 0.24 ng, 0.12 ng, 0.06 ng; rhBMP4 and rhBMP7: 0.96ng, 0.48 ng, 0.24 ng, 0.12 ng

(D) Treatment of hBMP4/4 homodimer with plasmin and thrombin results in altered gel mobility on silver stained SDS-PAGE and loss of immunoreactivity in western blot. Thrombin treatment results in a single smaller BMP4 band. Treatment with plasmin yields multiple cleavages. Time in hours refers to time of incubation with protease. (see also Figure S2C-D).

Fig. 3. Inhibition of BMP signaling via expression of dominant negative BMP receptors inhibits cell cycle re-entry *in vitro* and *in vivo*.

(A) Cultured newt myotubes electroporated with expression plasmids for the three dominant negative BMP receptors (dnALK2, dnALK3, dnALK6) together with nucGFP or nucGFP alone as control were stimulated with recombinant hBMP4/7 and then assayed for BrdU incorporation. Data are presented as mean \pm SEM (n = 9 and n = 15 in control and dnBMPR respectively). Significance calculated by Student's t-test.

(B) Schematic outline of the *in vivo* experiments. Dotted lines indicate the cross sections for immunostaining. Representative staining pictures from a dnALK6 overexpressed limb are shown in (C) and (D).

(C) YFP⁺ nuclei are MHC⁺ and EdU⁻ in the stump muscle.

(D) Dedifferentiated YFP⁺ nuclei in the blastema lose MHC and a fraction incorporates EdU. Arrows point to YFP⁺EdU⁻ cells. Arrowheads point to YFP⁺EdU⁺ cells.

(E) Overexpression of dnALKs in myofibers reduces the cell cycle entry of the dedifferentiated cells during limb regeneration. Data are presented as mean \pm SEM (n = 4). Significance calculated by Student's t-test.

Formatted: English (U.S.)

Formatted: English (U.S.)

Formatted: English (U.S.)

Fig. 4. Molecular analysis of BMP signaling events *in vitro* and *in vivo*

(A) Luciferase activity assay of Smad-reporter in A1 newt myotube cultures. Data are presented as mean \pm SEM (n=8). Significance calculated by Student's t-test.

(B) Luciferase reporter assay indicates increased SMAD signaling *in vivo* during the dedifferentiation stage of limb regeneration. The Smad-reporter and the Renilla luciferase control plasmids were electroporated into the uninjured newt limb, 5dpa and 11dpa blastemas. The luciferase activity was analyzed the next day. Data are presented as mean \pm SEM (n=5). Significance calculated by Student's t-test.

(C) Dedifferentiating muscle cells display nuclearly localized phosphoSMAD. Immunohistochemical detection of increased phospho-smad1/5/8 in blastema nuclei compared to the stump (top of left panel). White line marks the amputation plane. Arrow indicates the stump region with low level of pSMAD. Asterisk indicates the background fluorescence of the myofibers.

Inset (right) de-differentiating YFP-expressing myofibre progeny (green) have pSMAD⁺ nuclei (red). Arrowheads, YFP⁺pSMAD⁺ cells in the blastema. Scale bars, 200 μ m (overview) and 20 μ m (insert).

(D) Recombinant Δ N-BMP4 is more potent in inducing cell cycle reentry in cultured myotubes compared to full-length BMP4. FCS treatment was used as a positive control. Data are presented as mean \pm SEM (n = 3 in control and 6 in all the other treatments). Significance calculated by Student's t-test.

(E) Schematic representation of the experiment testing the potency of the Δ N-BMP4 during limb regeneration. Equal amounts of baculovirus expressing full length BMP4, Δ N-BMP4 or cherry was injected into the early blastema. Muscle cell proliferation was quantified by MCM2 staining in the YFP⁺ myofibre progeny at 13 dpa.

(F) Dedifferentiated YFP⁺ nuclei in the blastema proliferate. Arrows point to YFP⁺MCM2⁻ cells. Arrowheads point to YFP⁺MCM2⁺ cells.

(G) Both full length BMP4 and Δ N-BMP4 increase the fraction of proliferating myofibre derived cells but Δ N-BMP4 is more potent compared to full-length BMP4. Data are presented as mean \pm SEM (n = 8). Significance calculated by Student's t-test.

682

683 **EXPERIMENTAL PROCEDURES**

684 **CONTACT FOR REAGENT AND RESOURCE SHARING:**

685 Further information and requests for resources and reagents should be directed
686 to and will be fulfilled by the Lead Contact, Elly Tanaka (elly.tanaka@imp.ac.at)

687

688 **EXPERIMENTAL MODEL AND SUBJECT DETAILS:**

689 Red-spotted newts, *Notophthalmus viridescens*, were supplied by Charles D.
690 Sullivan Co. (Nashville, TN, USA). Animals were kept in tanks fill with tap water
691 at density of 4 animals/0.01m² and kept at 18-20°C with regular water change.
692 Aquaria contained environmental enrichments composed of ceramic pieces for
693 hiding and artificial plants. Animals were fed with frozen blood worms. Unsexed
694 animals were randomly assigned to experimental groups.

695 Cell line, from *Notophthalmus viridescens*, called the A1 cell line was passaged
696 and differentiated as described in Tanaka et al 1997. Newt myoblasts were
697 cultured in 62.5% MEM (Invitrogen), 10% fetal bovine serum (Perbio),
698 penicillin/streptomycin (Gibco) and glutamine (Gibco) on gelatin (Sigma) coated
699 dishes, at 25°C and 2% CO₂. Cells were trypsinized once per week and split 1:3
700 before plating on flasks (Corning or Nunc) coated with 0.75% porcine gelatin Sex
701 unknown. Cells not authenticated.

702 Human HEK293 cell line: Shaking cultures were maintained at 37°C, 8% CO₂ in
703 Freestyle293 serum-free medium (Thermo Fischer). Sex: female. Cells
704 purchased and not further validated in the laboratory.

705 Sf9 Cell line for baculovirus production: We used expresSF+ Cells

706 (ProteinSciences (Meriden, CT, USA), sex: unknown. BV recombinants were

generated upon co-transfection of linearized bacmid DNA and a rescue vector using expresSF+ cell line (Protein Sciences Corp.). Cultured cells were maintained under continuous rotation suspension culture at 25°C in ESF 921 Insect Cell Culture Medium (96-001, Expression Systems). Virions were subjected to two rounds of amplification previous to a final expansion, where 500 ml of expresSF+ cells at 0.6×10^6 cells/ml were infected with 500 µl of BV virion-containing supernatant. This final incubation proceeded for 4 days at 25°C under continuous rotation, after which baculovirus particles were concentrated and purified using a gradient separation method.

METHOD DETAILS

Purification/Chromatography.

Crude bovine thrombin (Celliance Corp) was reconstituted at 20 mg/ml in 20 mM cation buffer (6.6 mM HEPES, 6.6 mM MES, 6.6 mM NaAcetate (pH 6.5) and loaded onto a HiTrap CMFF column. The flow through was collected and remaining thrombin inhibited with D-Phe-Pro-Arg-chloromethylketone, HCL (PPACK, Calbiochem). The flow through was mixed with phosphate buffer (pH 7.0) and ammonium sulfate to a final concentration of 33.3 mM and 100 mM respectively and loaded onto a HiTrap ButylFF column. Bound proteins were eluted in 50 mM phosphate buffer pH 7.0 by a stepwise gradient of 10 CV 100 mM ammonium sulfate, 0 mM ammonium sulfate, 20% Ethanol and 40% Ethanol.

The fraction eluted at 20% Ethanol (Butyl20) was mixed with NaCl to a final concentration of 200 mM and loaded onto a HiTrap Heparin column. Bound protein was eluted with a linear gradient of NaCl (0 mM to 1000 mM). Fractions

eluted between 430 mM and 680 mM NaCl were pooled, concentrated by ultrafiltration (MWCO 30,000) and mixed with CAPS (pH 11) to a final concentration of 100 mM. After incubation at room temperature for 4 hours the material was applied to a Superdex 200 column and fractions were collected.

Immunoprecipitation.

As a starting point for the immunoprecipitation a fraction of an intermediate step of the purification was used (Butyl20). Butyl20 was concentrated and dialyzed into 1X PBS. In order to remove IgG, the material was incubated with ProteinG beads at room temperature for 1 hour. Beads were removed and Butyl20-ΔIgG was incubated at 4°C, overnight with a) Noggin-FC or b) anti-BMP4 antibody (goat, polyclonal, R&D) or c) anti-EGFP antibody (goat, polyclonal, P.E.P.) that had been linked covalently to ProteinG beads. The beads were harvested and washed with a) 1X PBS, 0.01% SDS or b)/c) 10 mM phosphate buffer (pH8). Bound proteins were eluted with a) a step gradient of 0.1% SDS, 0.5% SDS, 1% SDS in 1X PBS or b)/c) 100 mM Phosphate buffer (pH11.5), 10 µg/ml aprotinin, for neutralization phosphate buffer (pH6.8) was added to a final concentration of 100 mM

Preparative SDS-PAGE.

The concentrated eluate that was obtained from immunoprecipitation was mixed with 5X sample buffer w/o DTT, incubated at 37°C for 1 hour and loaded onto a 4%-20% Tris-Glycine gradient gel (Anamed). Electrophoresis was carried out at room temperature and 100 V in 1X SDS running buffer. Single gel slices were obtained and proteins were eluted using D-Tube dialyzer midi (Novagen). Elution was carried out in a horizontal electrophoresis chamber at room temperature, 100 V for 7 hours.

SDS-PAGE and western Blots.

Samples were mixed with 5X Sample Buffer (with or without DTT), incubated at 95°C for 5 min and loaded either onto 4%-20% Tris-Glycine gels (Anamed) or 12% Bis-Tris gels (NuPAGE). Electrophoresis was carried out either in 1X SDS running buffer or 1X MES-SDS running buffer (NuPAGE) at room temperature and 130 V. After blotting the membrane was blocked with 1X PBS, 2% BSA. Antibodies for western blot were reconstituted according to manufacture's advice and used at the following dilutions: BMP2 (rabbit, polyclonal, Acris antibodies) 1:1000, BMP4 (goat, polyclonal, R&D) 1:5000, BMP4 (goat, polyclonal, Santa Cruz) 1:1000, BMP5 (goat, polyclonal, R&D) 1:1000, BMP6 (goat, polyclonal, R&D) 1:1000, BMP7 (rabbit, polyclonal, Prepro Tech EC Ltd) 1:5000. As standards for western blot commercially available recombinant BMPs (R&D) were used.

De-glycosylation of samples.

Samples were denatured by adding SDS and DTT at a final concentration of 0.5 % and 20 mM respectively and subsequent heating to 95°C for 5 min. In the case of subsequent activity analyses the denaturing procedure was performed in the absence of DTT, at 37°C for 2 hours. After cooling to room temperature NP40 was added to a final concentration of 1%. The sample was mixed and 10X assay buffer (500 mM sodium phosphate, pH 7.5) was added to achieve a final concentration of 1X. The sample was then incubated with N-Glycosidase F (PNGase F) at a final concentration of 1200 U/ml (0.36 mg/ml) for 1 hour at 37°C.

Cell culture.

781 Newt myoblasts were cultured in 62.5% MEM (Invitrogen), 10% fetal bovine
782 serum (Perbio), penicillin/streptomycin (Gibco) and glutamine (Gibco) on
783 gelatine (Sigma) coated dishes, at 25°C and 2% CO₂. In order to induce myotube
784 formation, cells were placed into 0.5% serum medium for 5 to 6 days. Myotubes
785 were purified by sieving the trypsinized cell preparation through a 100 micron
786 mesh to remove large aggregates, then the flow-through was passed through a
787 35 micron mesh, which passed the contaminating mononucleates through but
788 trapped the myotubes. The myotubes were washed off of the sieves and plated
789 in 0.5% serum media on fibronectin coated 96-well plates (Tanaka, 1997).
790 Protein fractions usually in the presence of 0.5% serum medium were added to
791 cells 8 hours after cell preparation. Four days after adding of samples, cells were
792 labeled with bromodeoxyuridine (BrdU, Sigma) at a final concentration of 13
793 µg/ml. After 12 hours of labeling, cells were fixed and stained for BrdU as well as
794 the muscle marker myosin heavy chain (MHC) as described previously (Tanaka
795 et al., 1999). The percentage of MHC⁺/BrdU⁺ myotubes out of total MHC⁺
796 myotubes was determined using an Axioplan 2 imaging microscope (ZEISS). The
797 specific activity of SPRF was defined in Units where the amount of material
798 added to myotubes that resulted in a 1% BrdU⁺ myotube response in 150 µl of
799 culture media. In other words, if we added an amount of serum preparation of 10
800 µg protein /150 µl media that induced 10% of myotubes to take up BrdU, we
801 defined this as 1U SPRF/1µg protein added.

802 **Electroporation of newt myotubes.**

803 Newt myotubes from one cell culture dish (100 mm diameter) were harvested as
804 previously described (Tanaka et al., 1997). Cells were centrifuged (300 g, 3 min).
805 The cell pellet was re-suspended in 300 µl ice-cold 1X Steinberg's buffer and

806 transferred into a BTX electroporation device (pre-cooled to 4°C). 10 ug DNA
807 were added per sample. The electroporation was carried out using a square
808 pulse electroporator (BTX 830 Squarporator) at 75 V, 35 msec, for five pulses.
809 0.5% serum medium was added, myotubes were purified as described (Tanaka
810 et al., 1997) and plated on fibronectin coated 96-well plates.

811 **Cloning of BMP and noggin-FC constructs.**

812 Complete human cDNAs for human BMP4, human BMP7 and human Noggin were
813 obtained from the German Resource Center for Genome Research (RZPD). The
814 coding sequence of noggin was inserted into pSUPER-M1, a derivative of Signal
815 pIG-plus (R&D Systems) and p23 (a kind gift from Barbara Borgonovo) to
816 generate a CMV promoter driven construct expressing a C-terminal human IgG1
817 Fc domain fusion. Human BMP4 and BMP7 were sub-cloned into pCMV-M2, a
818 derivative of pCMVSPORT6 (Invitrogen). The bovine orthologs of human BMP4
819 and BMP7, human BMP4_S298P and human BMP7_S295G_M315V, as well as the
820 human ΔN-BMP4 mutant (lacking residues K3 to K14 of mature human BMP4)
821 were generated by site-directed mutagenesis using an overlap PCR protocol. All
822 constructs were verified by sequencing.

823 **Cloning of dnAlk constructs.**

824 Mutations for Alk2, 3, 6: dnAlk2 K235R, dnAlk3 K261R, dnAlk6 K231R.

825 Human Alk2, 3, 6 cDNAs were obtained from RZPD (now CellBioSource) and
826 coding sequences were PCR amplified to incorporate point mutants by standard
827 methods. PCR products were digested with NheI & EcoRI and ligated,
828 transformed in DH5alpha. A_Caggs-GFP vector was digested with NheI & EcoRI
829 and dnAlk sequences were inserted by ligation.

830 Generation of the Scel-mTol2-Caggs-lpCherry-H2B-YFP-T2A-dnAlk constructs.

The control plasmid (SceI-mTol2-Caggs-IpCherry-H2B-YFP-T2A-User) used in ((Sandoval-Guzman et al., 2014) were digested with BbvCI. Each dnAlk fragment was PCR amplified using Caggs-dnAlks for template and assembled by Gibson assembly (NEB). nucGFP was obtained from Clontech (eGFP-N2).

Expression of recombinant proteins

Recombinant proteins were expressed by transient transfection of suspension cultures of HEK293 cells and secreted into the medium. For the expression of BMP heterodimers expression constructs encoding the individual BMPs were co-transfected into HEK293 cells. Shaking cultures were maintained at 37°C, 8% CO₂ in Freestyle293 serum-free medium (Invitrogen). For transfection, plasmid DNA:PEI complexes, preformed at 10 µg/mL DNA and 100 µg/mL PEI (Polysciences, linear 25kD, #23966) in 150 mM NaCl were diluted 1:10 into cells adjusted to 2 x 10⁶/ml. After shaking incubation for 4 hours, the medium was replaced and the cultures diluted to 1 x 10⁶ cells/ml. After shaking for 4 days, conditioned medium was harvested by centrifugation (500 x g, 5 min), sterile filtered (0.2 µM), concentrated using Amicon Ultra-15 centrifugal filter units (Millipore), and dialyzed into PBS. Bacterially expressed recombinant human BMP4/4 used for mass spectrometry analysis was a kind gift from Walter Sebald. Bacterially expressed recombinant human BMP4/4 and BMP4/7 used for Edman sequencing were purchased from R&D.

BMP Inhibition.

The sample was mixed with noggin-FC or antibody and incubated at room temperature for 1 hour before loading on myotubes.

Plasmin/Thrombin Digest.

856 If not stated differently the digests for cell assay samples was performed in 50
857 mM Tris, 150 mM NaCl, pH7.4 (plasmin) or 50 mM Tris, 150 mM NaCl pH8.3
858 (thrombin) buffer. Plasmin (Enzyme Research Labs) or thrombin (Enzyme
859 Research Labs) were added to the sample at 16 ug/ml final concentration (molar
860 ratio protease:BMP = 1:10) and incubated at 37°C for 4 hours. In order to inhibit
861 proteolytic activity after incubation, PPACK was added to a final concentration of
862 4 µg/ml. As a quality control, before usage, the activity and specificity of plasmin
863 and thrombin was shown by digesting their specific substrates, ChromozymPL
864 and ChromozymTH (Boehringer-Mannheim) respectively. Plasmin digestion of
865 bacterially expressed recombinant hBMP4/4 for mass spectrometry analysis was
866 performed in 20 mM ammonium carbonate, 4 mM Hepes, 4 mM NaAcetate at
867 37°C for 15 minutes, 3 hours and 24 hours with a molar ratio of plasmin:BMP4/4
868 of 1:60.

869 **Mass spectrometry.**

870 Gel separated proteins were reduced, alkylated and in-gel digested with trypsin
871 as described in (Shevchenko et al., 2006). After digestion, peptides were twice
872 extracted with 50 µl of 5% formic acid and 50% acetonitrile, dried down, re-
873 dissolved in 20 µL of 5 % (v/v) formic acid and analyzed by mass spectrometry.
874 LC-MS/MS analysis of peptide mixtures was carried out on an Ultimate nanoLC
875 system (Dionex, Amsterdam, The Netherlands) interfaced on-line to a LTQ linear
876 trap mass spectrometer (Thermo Fisher Scientific, San Jose) (Waridel et al.,
877 2007). Acquired MS/MS spectra were searched against a comprehensive NCBI
878 protein sequences database using MASCOT software (Matrix Science, v.2.2.0)
879 installed on a local server under the following settings: mass tolerance was set as
880 2 Da for peptide masses and 0.5 Da for masses of peptide fragments; variable

881 modifications: Propionamide (C), Carbamidomethyl (C), N-acetylation (Protein
882 N-terminus), Oxidation (M); enzyme: trypsin; two missed cleavages were
883 allowed. All hits with peptide ions scores above 25 were manually evaluated.

884 **MS analysis of plasmin treated bacterially produced recombinant**
885 **hBMP4/4.**

886 Plasmin digestion was performed in 10 mM Ammonium bicarbonate. One aliquot
887 of the sample (5 µl) was acidified (1 µl 30% formic acid) and after addition of 20
888 µl of 80% acetonitrile solvent was evaporated in a speed vac (non-reduced
889 sample). A second aliquot of the sample (5 µl) was acidified (1 µl 30% formic
890 acid) to stop digestion, neutralized with ammonium bicarbonate and reduced
891 with 10 mM DTT (2 hours at 37°C) and alkylated with 50 mM iodacetamide (1.5
892 hours at room temperature in the dark). Excess of iodacetamide was captured by
893 a second addition of 10 mM DTT and further incubation for 1 hour at room
894 temperature. After addition of 20 µl of 80% acetonitrile solvent was evaporated
895 in a speed vac and dry samples were stored at -20°C until analysis. For HPLC-
896 MS/MS analysis samples were separated in a linear gradient of
897 water/acetonitrile with 0.1% formic acid on a 75 µm i.d. C-18 Acclaim capillary
898 column (Dionex, Idstein, Germany) at a flow rate of 200 nl/min with an Eksigent
899 2D Nano-LC system (Eksigent, Dublin, CA, USA). The HPLC system was
900 hyphenated via a TriVersa Nanomate automatic source (Advion, Ithaca, USA) to
901 an Orbitrap-Velos mass spectrometer (Thermo Fisher Scientific, Bremen,
902 Germany) operated in data-dependent acquisition mode with a nominal
903 resolution of 60000 at 400 m/z and lock mass enabled for MS spectra and
904 MS/MS acquisition in the Velos ion trap.

905 **Animal procedures**

906 Red-spotted newts, *Notophthalmus viridescens*, were supplied by Charles D.
907 Sullivan Co. (Nashville, TN, USA). Plasmid preparation injection, and
908 electroporation were carried out as in (Sandoval-Guzman et al., 2014). Animals
909 were anesthetized in 0.1% ethyl 3-aminobenzoate methanesulfonate (Sigma) for
910 15 min. Forelimbs were amputated above the elbow, and the bone and soft tissue
911 were trimmed to produce a flat amputation surface. Animals were left to recover
912 overnight in an aqueous solution of 0.5% sulfamerazine (Sigma). At specified
913 time-points, the regenerating limbs were collected. Three μ l of 5mg/ml AEBSF
914 (Roche) and/or baculo virus expressing BMP4 or cherry was injected into the
915 blastema at 6dpa and 9dpa. For EdU-labelling, animals were injected
916 intraperitoneally with 50-100 μ l of 1mg/ml EdU. All surgical procedures were
917 performed according to the European Community and local ethics committee
918 guidelines.

919 **Luciferase assay**

920 Smad-luc reporter (pGL3-BRE-"BMP Responsive Element"-Luciferase plasmid)
921 was from Addgene, pGL3-basic and pRL-Renilla were from Promega. Dual
922 Luciferase Assay system (Promega) was used to measure the luciferase activity
923 in A1 myotubes, and in limbs. An Amaxa Nucleofector was used for
924 electroporation of A1 myoblasts (Program T30) and the myoblasts were
925 differentiated into myotubes over 7 days. Recombinant BMP4/7 with or without
926 noggin was added into the cultured myotubes (500ng/ml). A1 myotubes were
927 lysed after 24h using the passive lysis buffer provided in the dual luciferase
928 reporter assay kit following the manufacturer's instructions. The *in vivo*
929 luciferase analysis procedures were modified from (Yun et al, 2013). In short,
930 Smad-luc and pRL-Renilla plasmids were mixed at 10 μ g/ μ l. Three or 5 μ l of

plasmid solutions were injected into blastemas or uninjured limbs, respectively. Electroporations were performed by NEPA21 electroporator with parallel fixed platinum electrodes using 10 pulses (duration: 100ms, voltage: 30volts decending). Tissues were collected 24h after electroporation and immediately homogenized in passive lysis buffer (Promega).Lysates were centrifuged to remove debris, and assayed according to the dual luciferase reporter protocol. The activities of the Smad-Luc reporter were normalized to the activity of the internal Renilla control and expressed as relative luciferase activity (Firefly/Renilla).

Baculo virus production

Production of pseudotyped baculovirus was as described in Nacu et al 2016. Baculovirus was pseudotyped with vsv-ged gene, which was inserted into the rescue vector under the baculovirus polyhedrin promoter.BMP4 or Cherry constructs were cloned into a rescue vector using standard restriction enzyme methods, and are expressed under the control of a CMV promoter. The generation of baculoviruses was carried out by co-transfection of the above-mentioned rescue vector together with replication incompetent baculovirus DNA into SF9 ESF insect cell line. Upon culture expansion, recombinant baculovirus particles were collected, concentrated and purified using the sucrose gradient separation method. The titer was assessed in SF9ET cells, by means of end-point dilution assay.

Immunohistochemistry

Frozen sections (8 μ m) were thawed at room temperature and fixed in 4% formaldehyde for 5 min. Sections were blocked with 5% donkey serum and 0.1% Triton-X for 30 min at room temperature. Sections were incubated with anti-GFP

(Abcam 6673) and anti-MHC (DSHB) or anti-Phospho-Smad1/5/8 (Cell Signaling 9511) overnight at 4°C and with secondary antibodies for 1 hour at room temperature. Antibodies were diluted in blocking buffer and sections were mounted in mounting medium (DakoCytomation) containing 5 µg/ml DAPI (Sigma). PhosSTOP (Roche) was used during Phospho-Smad1/5/8 staining process. EdU detection was performed according to (Salic and Mitchison, 2008). An LSM 700 Meta laser microscope with LSM 6.0 Image Browser software (Carl Zeiss) was used for confocal analyses. One in every 6 (Figure 3) or 10 (Figure 4) sections was selected and counted.

QUANTIFICATION AND STATISTICAL ANALYSIS

Error bars represent SEM unless otherwise indicated. Statistical analysis was performed using GraphPad Prism software.

Analysis of in vitro myotube cell cycle entry data:

The percentage of BrdU⁺ myotubes were counted and always presented as mean±SEM from n samples. In Figure 1C the sample size was n = 9 samples for each condition. Each sample was derived from counting one separate well containing a median of 84 myotubes per well. In Figure 1E the sample size was n = 9 samples (SPRF, PrG bead dep. and SPRF, αBMP4 + PrG bead dep.) and n = 54 samples (αBMP4 eluate). Each sample was derived from counting one separate well containing a median

978 of 44 myotubes per well. In Figure 3A the sample size was $n = 9$ samples
979 (control) and $n = 15$ samples (dnBMPR). Each sample was derived from
980 counting one separate well containing a median of 41 myotubes per well.
981 In Figure 4D the sample size was $n = 3$ in control and $n = 6$ in other
982 treatments. Each sample was derived from counting of one separate well
983 containing a median of 132 myotubes. The statistical significance was
984 always analyzed by an unpaired, two-tailed Student's t-test, (95%
985 confidence intervals). Please refer to figures for p-values.

986

987 Analysis of immunofluorescence staining data:

988 The percentages of $\text{EdU}^+/\text{YFP}^+$ cells were counted and presented as
989 $\text{mean} \pm \text{SEM}$, $n = 4$ limbs (Figure 3E), 8 limbs (Figure 4G), 6 limbs in
990 PBS and 8 limbs in AEBSF (Figure S4B), 8 limbs (Figure S4C) per each
991 treatment group. The statistical significance was analyzed by Student's t-
992 test, (95% confidence intervals). Please refer to figures for p-values.

993

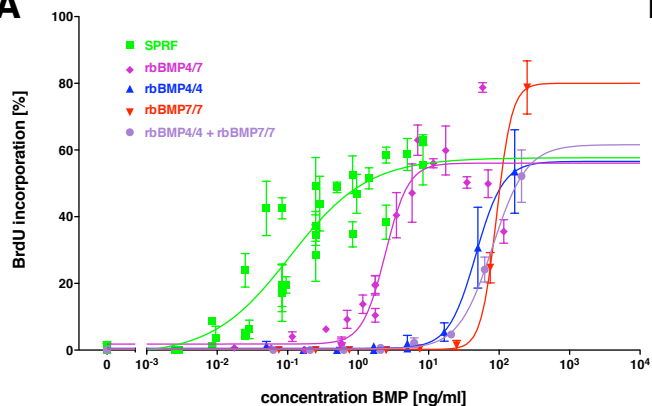
994 Analysis of luciferase activity data:

995 The in vitro luciferase activity data were presented as $\text{mean} \pm \text{SEM}$, $n = 8$
996 samples (Figure 4A). Each plate contained 10^6 cells and triplicate plates
997 were averaged for each sample. The in vivo luciferase activity data were
998 presented as $\text{mean} \pm \text{SEM}$, $n = 5$ limbs per each group (Figure 4B). The

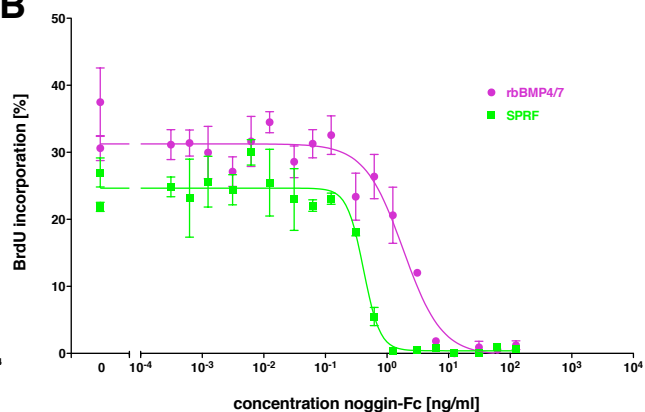
999 statistical significance was analyzed by Student's t-test, (95% confidence
1000 intervals). Please refer to figures for p-values.
1001
1002

Figure 1

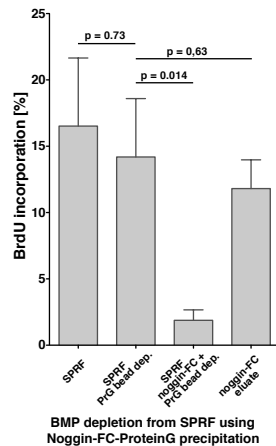
A



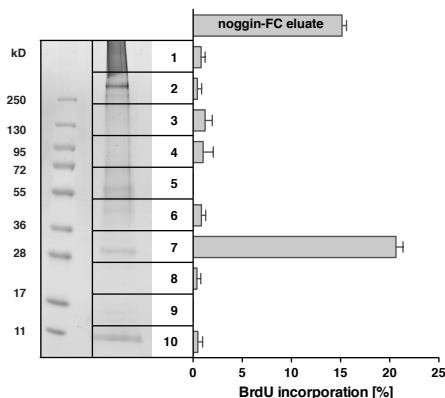
B



C



D



E

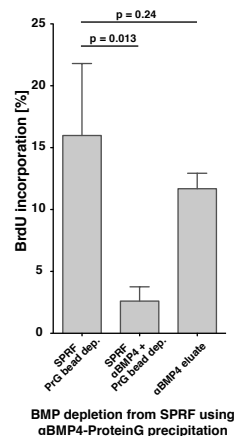
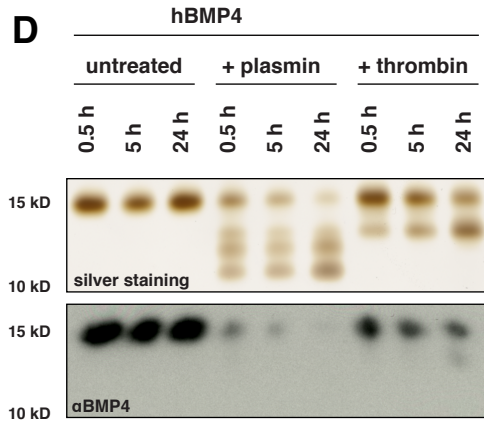
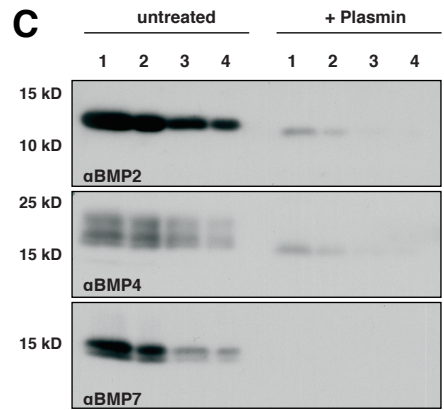
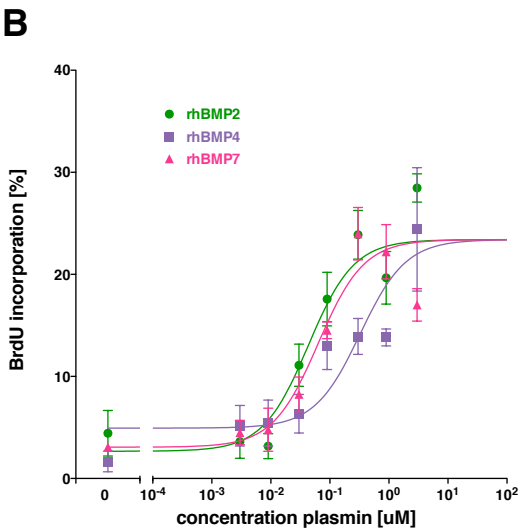
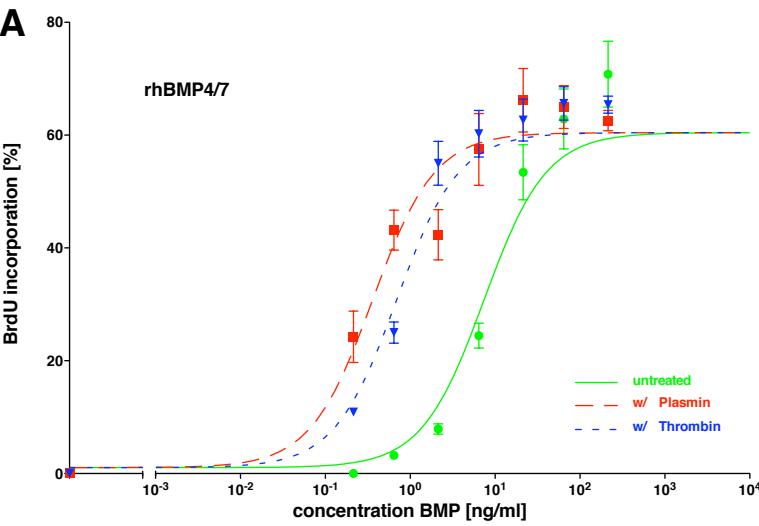
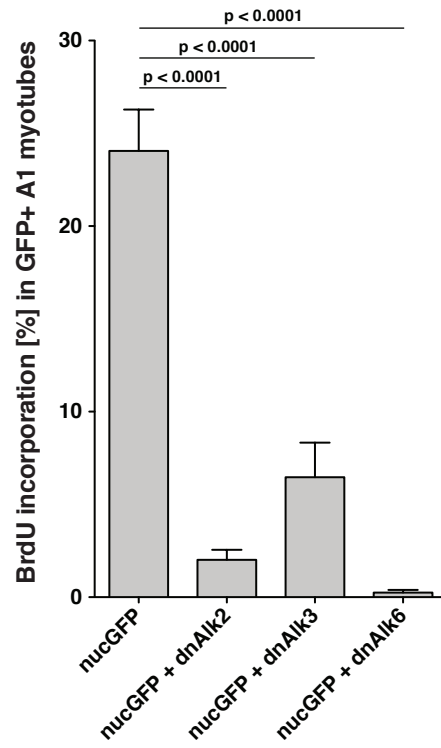
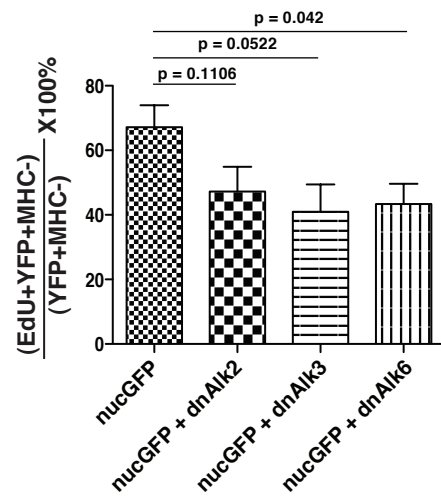
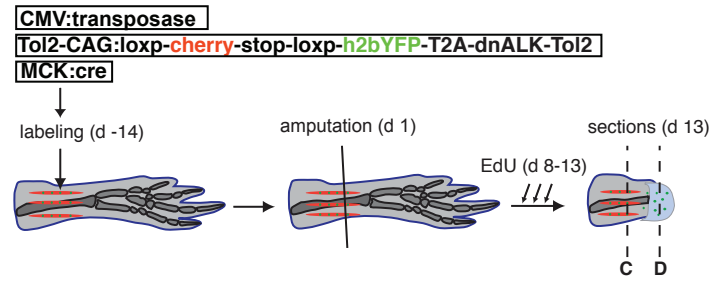
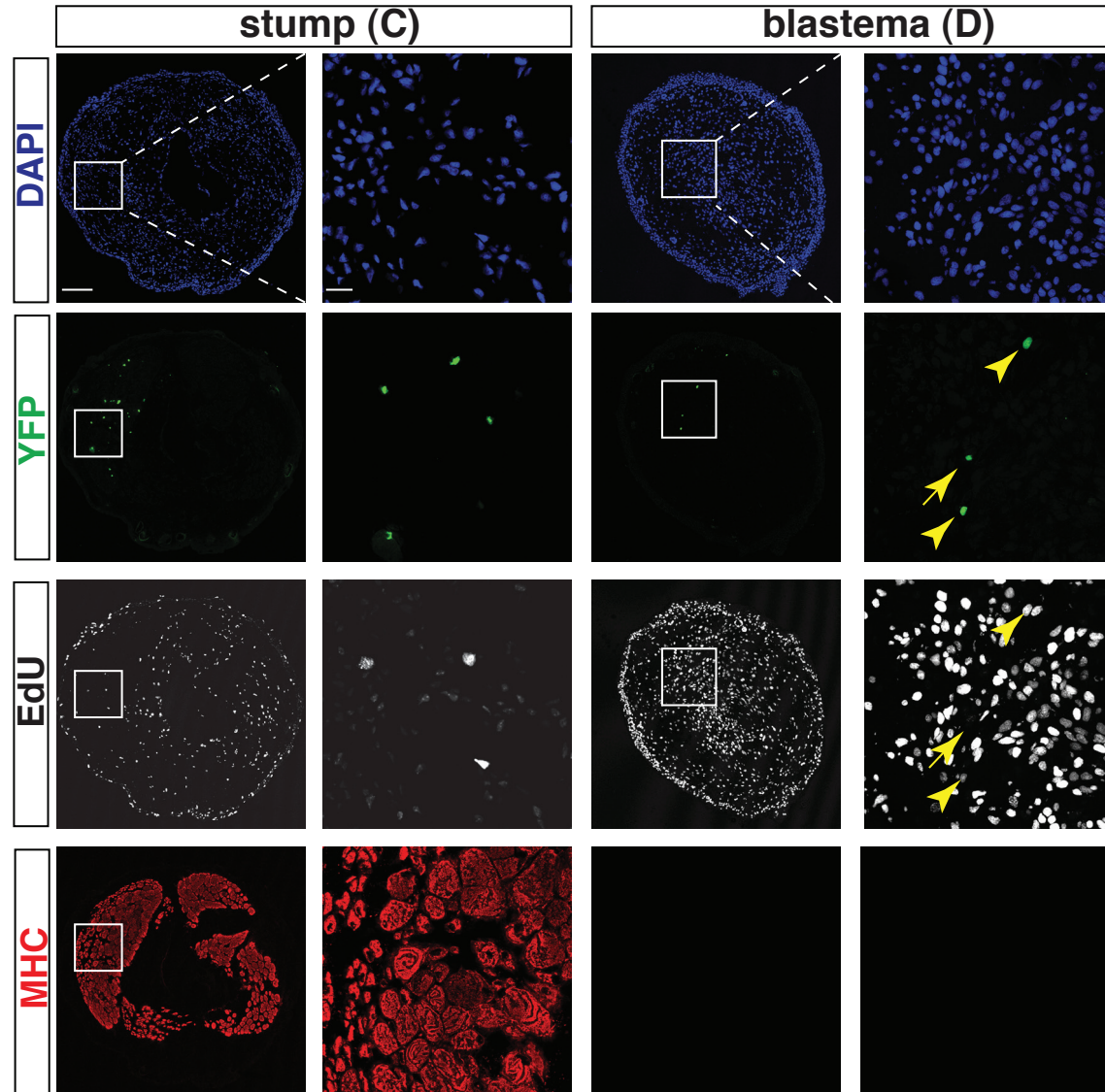
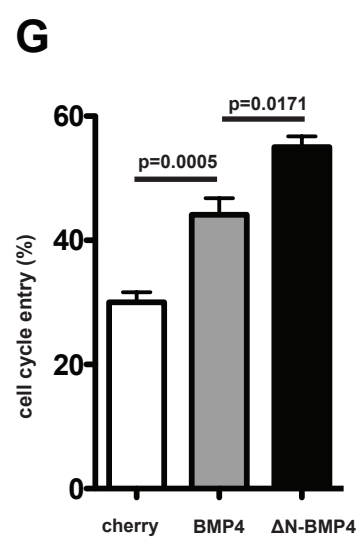
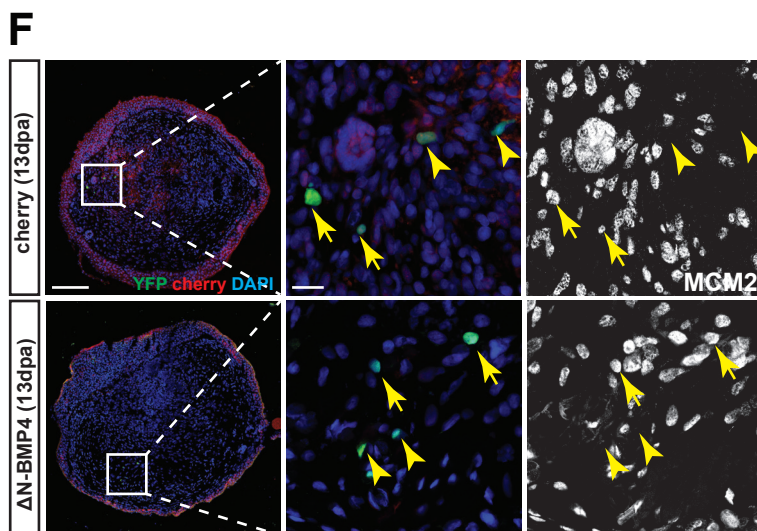
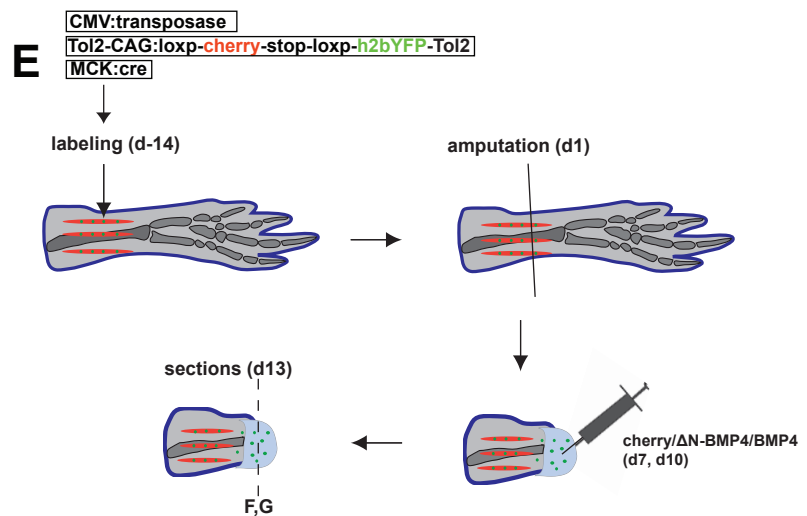
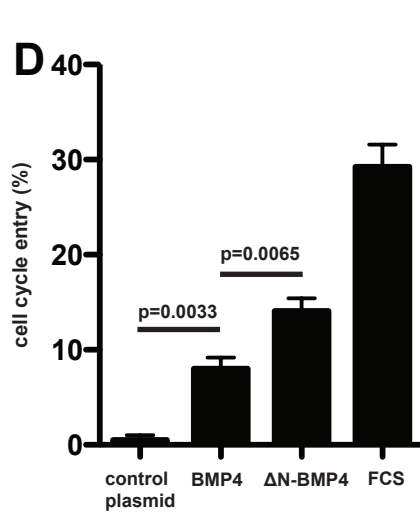
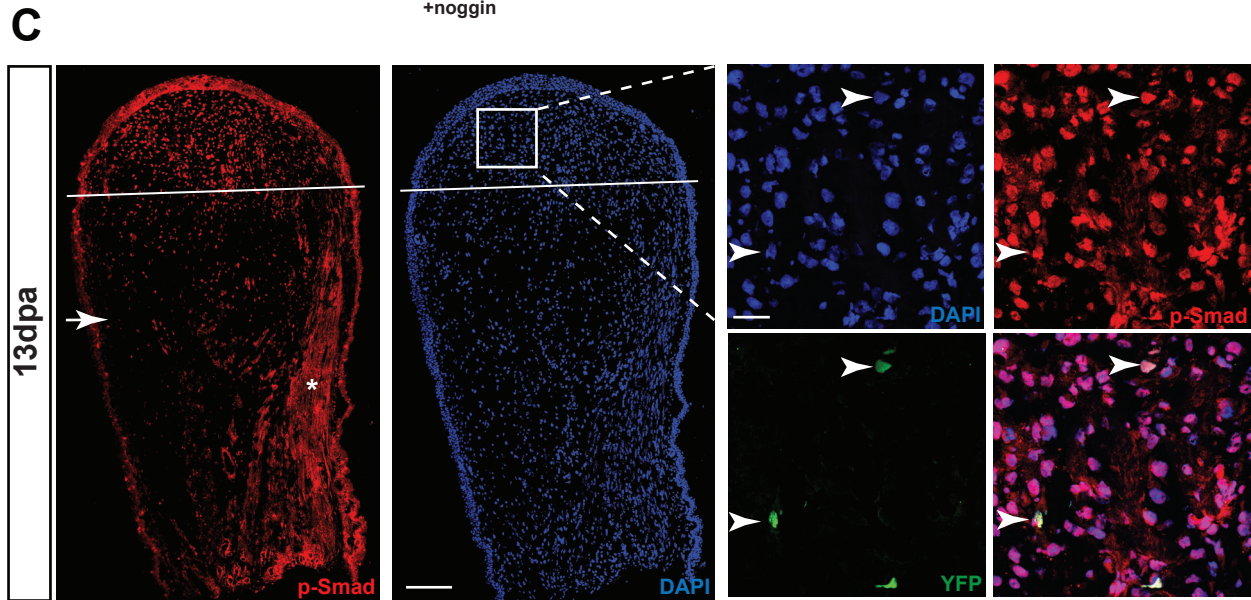
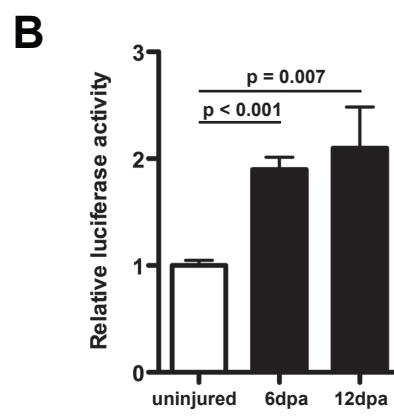
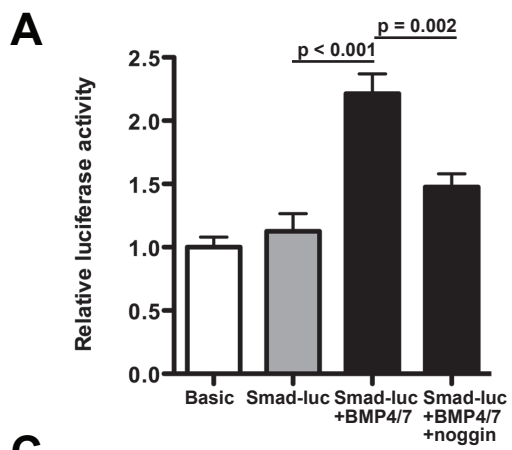


Figure 2



A**E****B****CD**



Inventory of Supplemental Information

Supplemental Figures

Figure S1. Bovine BMP4 co-fractionates with serum-derived myotube S-phase re-entry inducing activity. Relates to Figure 1.

Figure S2. Serum BMPs are more potent than recombinant BMPs under serum-free conditions, BMP signaling is required for S-phase re-entry of newt myotubes and the potency of recombinant BMPs is increased after thrombin and plasmin treatment. Relates to Figure 1 and Figure 2.

Figure S3. Mapping the target sites for thrombin and plasmin in hBMP4/4 by Edman sequencing. Relates to Figure 2, Data S1 and Table S2.

Figure S4. Serine proteases act upstream of BMPs to promote cell cycle entry of dedifferentiating myofibers. Relates to Figure 4.

Supplemental Tables

Table S1. Bone morphogenetic proteins identified in BMP4 immunoprecipitation by mass spectrometry. Relates to Figure 2.

Supplemental Tables (separate .xlsx files)

Table S2. Edman sequencing of rhBMPs. Relates to Figure 2 Figure S3 and Data S1.

Table S3. Bovine BMP peptides identified by mass spectrometry. Relates to Figure 1 and Figure S1.

Supplemental Data (separate .pdf file)

Data S1. Traces of Edman sequencing of rhBMPs. Relates to Figure 2, Figure S3 and TableS2.

Supplemental Figures

Figure S1

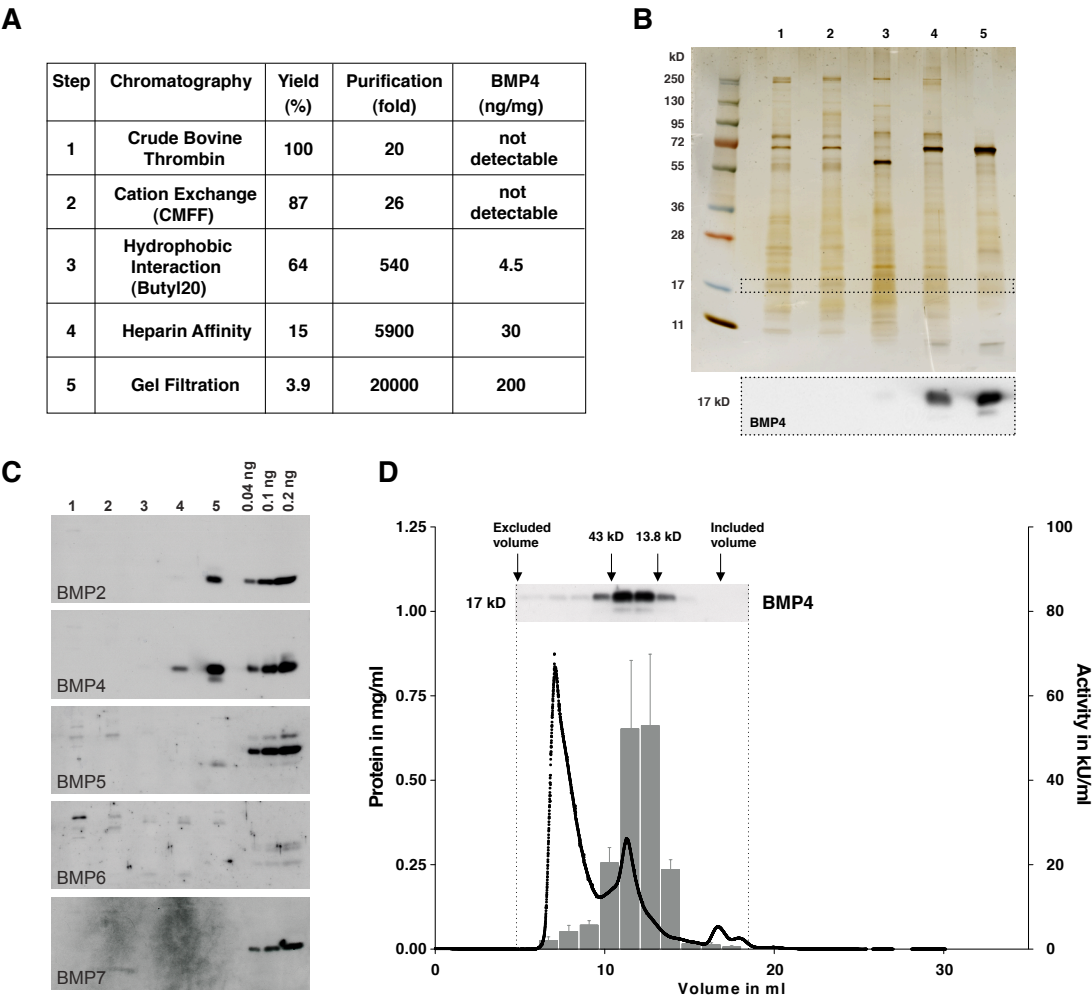


Figure S1. Bovine BMP4 co-fractionates with serum-derived myotube S-phase re-entry inducing activity. Relates to Figure 1.

(A) Summary of purification steps and -fold enrichment of activity across the purification. Specific activity of pooled peak fractions from each column step was measured as the described in Materials and Methods based on the myotube bioassay. The “fold purification” was calculated based on the fold increase in specific activity found in the peak pool from each chromatography step and “yield” was calculated based on the total amount of activity found in the peak pool from each step. BMP4 was quantitated by western blot using commercial recombinant hBMP4/4 as standard protein.

(B) Top: silver stained reducing gel of peak fractions from the five column steps listed in (A). Equal amount of protein were loaded in each sample. Dotted lines at 17

kD mark the region of the gel shown in the western blot below. Bottom: anti-BMP4 western blot of samples shows enrichment of BMP4 across the purification.

(C) The indicated BMPs were detected by western blotting. 1-5: peak activity fractions of single purification steps: (1) Crude Bovine Thrombin - starting material (2) Cation Exchange Chromatography (3) Hydrophobic Interaction Chromatography (4) Heparin Affinity Chromatography (5) Size Exclusion Chromatography. For each fraction 1 µg total protein was used in reducing conditions. 0.04 ng, 0.1 ng and 0.2 ng of respective BMP standards were loaded in control lanes.

(D) Co-fractionation of BMP4 with activity during gel filtration fractionation. Protein elution profile (black line), activity profile (gray bars), and BMP4 immunoblotting across the gel filtration column (purification step 5) shows that BMP4 co-fractionates with the activity. The elution volumes of protein standards are indicated at the top of the chart. Fractions that eluted within the markers for the excluded volume (blue dextran, 2000 kD) and the included volume (salt peak) were analyzed. Amongst others, ovalbumin (43 kD) and ribonuclease A (13.8 kD) were used as molecular weight standards. For western blotting, pools from three consecutive fractions were prepared and equal volumes of pooled fractions were separated by SDS-PAGE in reducing conditions. The S-phase re-entry activity for the pooled samples was calculated by averaging the activity that was found from individually assaying the single fractions of each pool on newt myotubes.

Figure S2

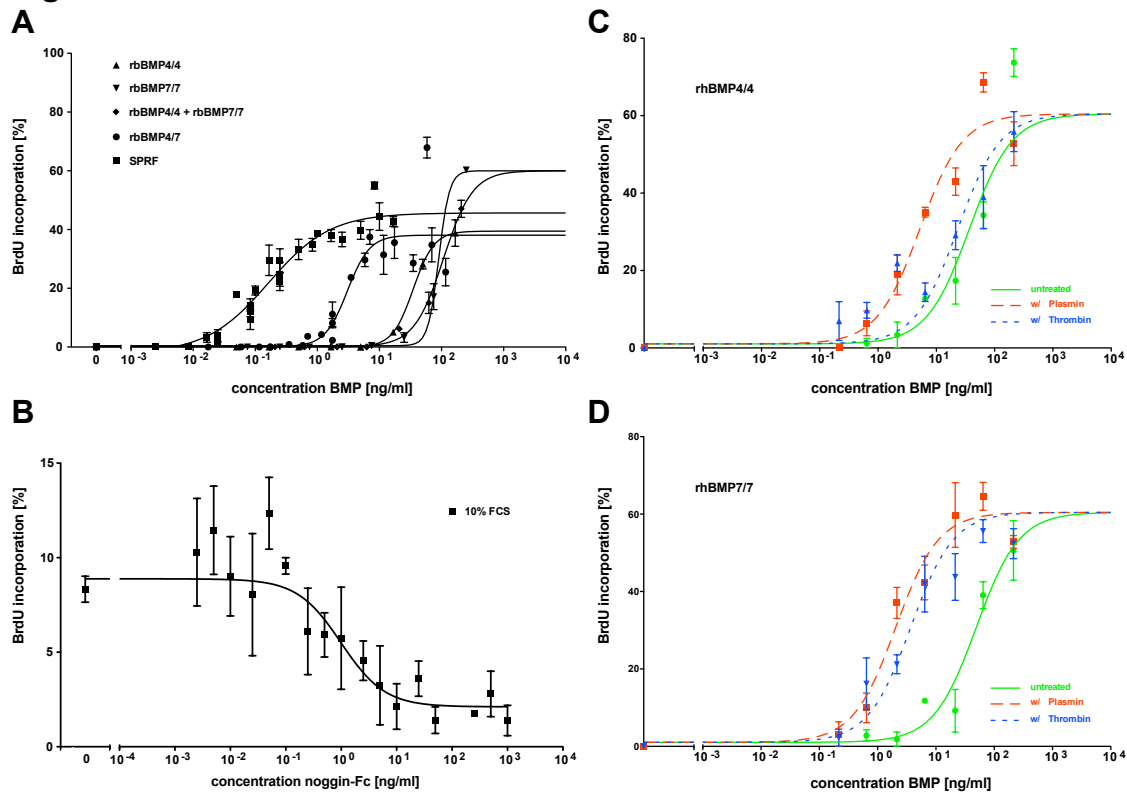


Figure S2. Serum BMPs are more potent than recombinant BMPs under serum-free conditions, BMP signaling is required for S-phase re-entry of newt myotubes and the potency of recombinant BMPs is increased after thrombin and plasmin treatment. Relates to Figure 1 and Figure 2.

(A) Dose response curves under serum-free conditions for recombinant bovine BMP4/4, BMP7/7 and BMP4/7 containing dimers produced by transfection of 293 cells compared to dose response for serum-derived bovine BMP4-containing dimers. BMP4 protein was quantitated by western blotting against a standard purified protein preparation. Square: Serum-derived BMP2 and BMP4 (SPRF), Circle: recombinant BMP4/7 heterodimer, Diamond: recBMP4/4 plus recBMP7/7 mixture, Inverted triangle: recBMP7/7, Triangle: recBMP4/4. Data are presented as mean \pm SEM (n = 3).

(B) Noggin inhibits the S-phase re-entry activity in fetal calf serum (FCS). Inhibition of S-phase re-entry by addition of recombinant human noggin-Fc, produced by transfection of HEK293 cells, to FCS. Data are presented as mean \pm SEM (n = 3).

(C) Dose response of untreated recombinant human BMP4/4 homodimer (circle, green, solid line) and after treatment with thrombin (triangle, blue, dotted line) or plasmin (square, red, dashed line). Data are presented as mean \pm SEM (n = 3).

(D) Dose response of untreated recombinant human BMP7/7 homodimer (circle, green, solid line) and after treatment with thrombin (inverted triangle, blue, dotted line).

line) or plasmin (square, red, dashed line). BMPs are made in HEK293 cells. Data are presented as mean \pm SEM (n = 3).

Figure S3. Mapping the target sites for thrombin and plasmin in hBMP4/4 by Edman. Relates to Figure 2, Data S1 and Table S2.

(A) N-terminal peptides found along the BMP4 and BMP7 sequences after Edman degradation analysis of BMP4/4 and BMP4/7. The N-terminus of untreated hBMP4/4 was verified in reducing conditions (pink - SPKHH). Thrombin-treated hBMP4/4 homodimer in the presence of DTT detected one main sequence ARKKN (green) suggesting cleavage at R8. The plasmin treated BMP4/4 yielded two major N-termini, KKNKN and NYQEMVV. In the plasmin treated hBMP4/7 heterodimer five main sequences (orange) NYQEMVV and KKNKNCR, as well as MANVAEN, DLGWQDW and NMVVRAC were found, indicating that plasmin targets hBMP4 at R10 and K103, whereas BMP7 is targeted at R22, R48 and R129.

(B) Samples from panel (C) were applied to SDS-PAGE in the presence or absence of DTT. For identification of hBMP4 versus hBMP7 peptides in hBMP4/7-derived samples, hBMP4/4 - untreated or after protease treatment - was run as a size standard in reducing conditions. Arrows indicate hBMP peptides (black = hBMP4/7 heterodimer peptides, blue = hBMP4 monomeric peptides, red = hBMP7 monomeric peptides). As shown by silver staining in reducing conditions (+DTT), in the case of BMP4, thrombin (T) gives rise to a single band, suggesting a single cleavage event. In contrast plasmin (P) cleavage results in two bands, suggesting multiple cleavages. In the case of BMP7, both thrombin and plasmin give rise to two bands each. However, thrombin and plasmin derived bands run at different molecular weights, indicating different specificity of the proteases.

(C) Activity assay of bacterially expressed BMP4/7. Bacterially expressed and purified recombinant hBMP4/7 was incubated with or without proteases (plasmin or thrombin). The specific activity of untreated and protease treated hBMP4/7 was measured in the newt myotube assay. Data are presented as mean \pm SEM (n = 3).

(D) Multiple sequence alignment of human BMP2, BMP4, BMP5, BMP6 and BMP7. BMPs are sub-grouped according to their sequence homology.

Mature bovine BMP2 and BMP4 display sequence similarity. Mature bovine BMP5, BMP6 and BMP7 display sequence similarity. The alignments of mature bovine BMP protein sequences were obtained from using the ClustalW2

(<http://www.ebi.ac.uk/Tools/services/web/toolform.ebi?tool=clustalw2>)

algorithm with standard parameters.

(E) Cartoon of mature human BMP4/4 homodimer. Arginine (R) and Lysine (K) residues are enlarged. BMP4 Monomers are connected by an intermolecular disulfide bond (brown dashed line) at Cysteine (C) C81. Three intramolecular disulfide bonds (green, dashed lines) are formed between C16-C80, C45-C113, C49-C115 in each of the monomers.

Figure S4

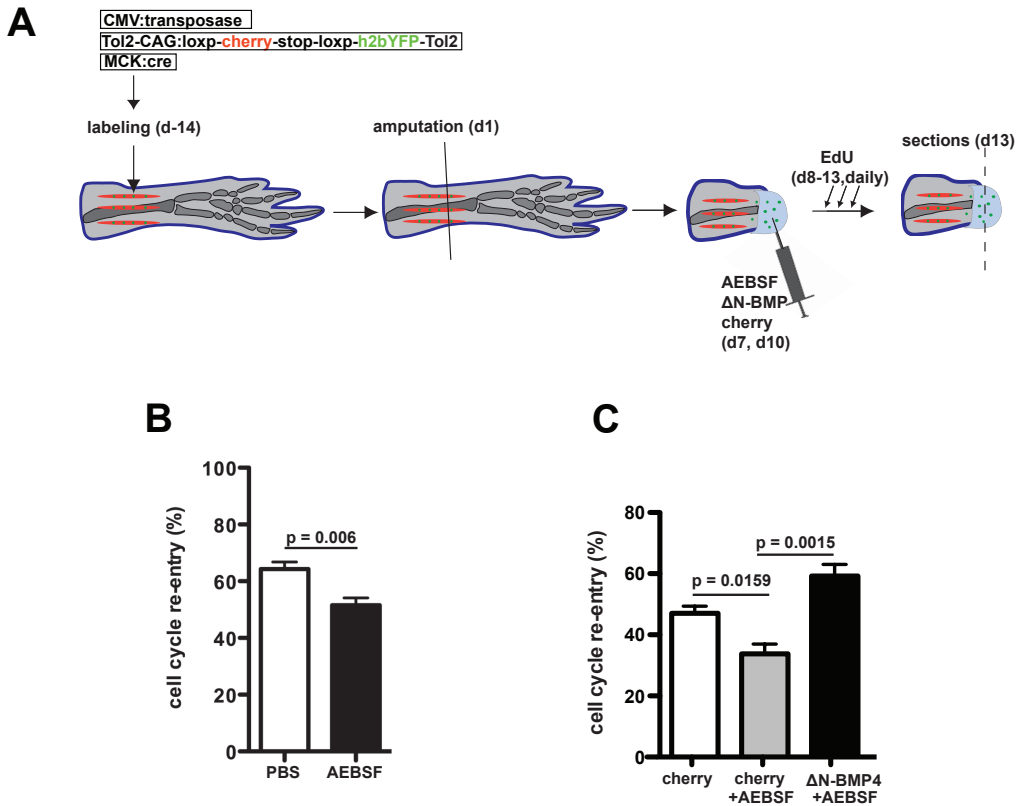


Figure S4. Serine proteases act upstream of BMPs to promote cell cycle entry of dedifferentiating myofibers. Relates to Figure 4.

(A) Representation of the experiment testing the effect of protease inhibition and BMP rescue on muscle dedifferentiation in vivo. The plasmin/thrombin inhibitor AEBSF or control PBS was injected together with baculovirus overexpressing Δ N-BMP4 or Cherry into the blastema at 6dpa and 9dpa. Cell-cycle re-entry was quantified by EdU incorporation in the YFP+ myofiber progeny at 13dpa.

(B) AEBSF reduces the cell-cycle re-entry of YFP+ cells in the blastema. Data are presented as mean \pm SEM (n = 6-8 limbs). Significance calculated by Student's t-test.

(C) Viral-mediated overexpression of Δ N-BMP4 rescues the suppression of muscle cell cycle re-entry by AEBSF-mediated protease inhibition. Data are presented as mean \pm SEM (n = 8 limbs). Significance calculated by Student's t-test.

Supplemental Tables

Table S1

N	Protein Name	Gene Identifier(s)	Peptides Detected by Mass Spectrometry		
			Sequence*	m/z	MASCOT peptide ions score
1	Bone Morphogenetic Protein 2	gi 7c149642861 gi 7c148744883 gi 7c157279020 gi 7c296481187 gi 7c153850483	K.NYQDMVVEGCGCR.-	802.5	64
2	Bone Morphogenetic Protein 4	gi 7c57545008 gi 7c68445390 gi 7c114052743 gi 7c109818952 gi 7c86821122 gi 7c296483082	K.NYQEMVVEGCGCR.- K.NYQEMVVEGCGCR.-	801.5 809.3	85 63
3	Bone Morphogenetic Protein 5	gi 7c194677539 gi 7c297488876 gi 7c296474598	K.LNAISVLYFDDSSNVILK.K R.MSSVGDYNTSEQK.Q R.MSSVGDYNTSEQK.Q K.KHELYVSFR.D** K.HELYVSFR.D**	1006.3 723.6 731.6 394.0 526.0	70 89 91 36 33
4	Bone Morphogenetic Protein 6	gi 7c194677896 gi 7c297489529 gi 7c296473962	R.ASSASDYNSSSELK.T	680.1	64
5	Bone Morphogenetic Protein 7	gi 7c76633049 gi 7c297481860 gi 7c296480909	R.VANVAENSSSDQR.Q K.KHELYVSFR.D** K.HELYVSFR.D**	689.1 394.0 526.1	84 36 33

Table S1. Bone morphogenetic proteins identified in BMP4 immunoprecipitation by mass spectrometry. Relates to Figure 2.

(*) M refers to methionine oxidized and C refers to cystein carbamidomethylated.

(**) Stretches are identical in BMP5 and BMP7 sequences.

Supplemental Tables (separate .xlsx files)

Table S2. Edman sequencing of rhBMPs. Relates to Figure 2 Figure S3 and Data S1.

Numerical data derived from Edman sequencing trace seen in Data S1 of rhBMP4/4 untreated/+plasmin/+thrombin as well as rhBMP4/7 + plasmin are presented for individual Edman cycles (1-5).

Table S3. Bovine BMP peptides identified by mass spectrometry. Relates to Figure 1 and Figure S1.

Table of the 34 proteins identified by MS from the gel slice of the final purification step. Peptides were identified by mass spectrometry of a non-reducing gel slice spanning 28-39 kD. Bovine BMP peptides that were identified mapped onto protein sequences of the complete precursor protein.

Supplemental Data (separate .pdf file)

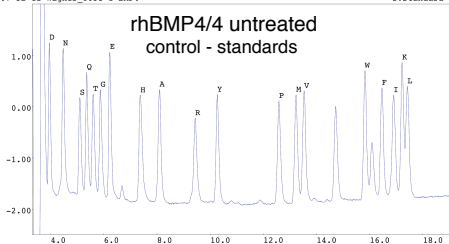
Data S1. Traces of Edman sequencing of rhBMPs. Relates to Figure 2, Figure S3 and TableS2.

Edman traces of rhBMP4/4 untreated/+plasmin/+thrombin as well as rhBMP4/7 + Plasmin are shown for individual Edman cycles (1-5). Colored circles (red, green, orange, blue, pink) highlight major amino acid peaks identified for each individual cycle. The corresponding colored circles in successive traces delineate a peptide that matches a BMP peptide sequence. Black circles highlight minor abundance amino acids that could not be assigned to the BMP query sequence and are most likely contamination.

Data S1

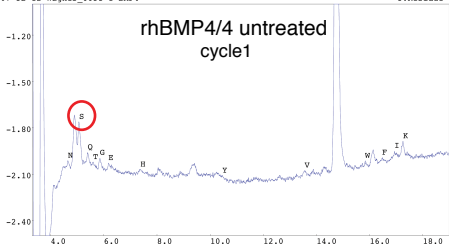
307-5B-12 Wagner_6631-1 BMP4

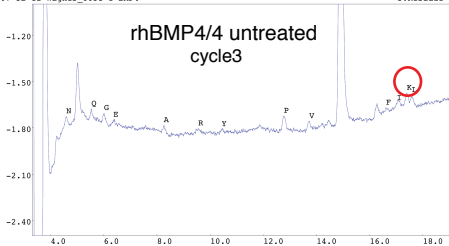
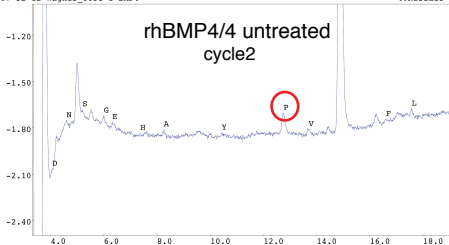
2:Standard 1

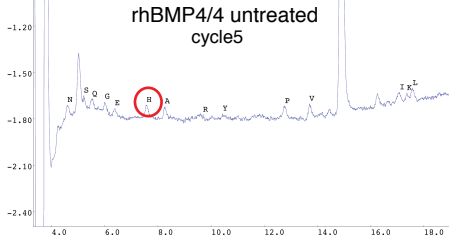
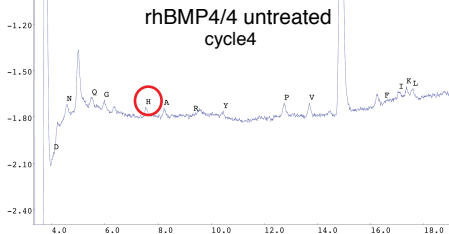


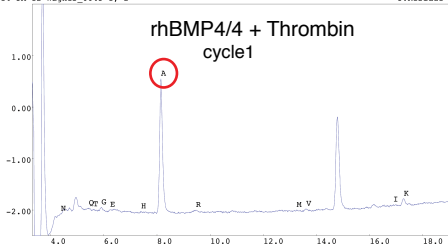
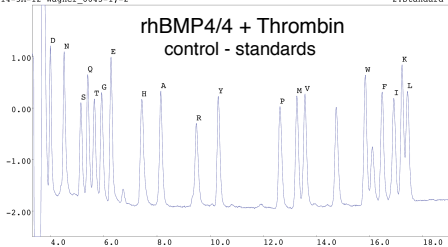
307-5B-12 Wagner_6631-1 BMP4

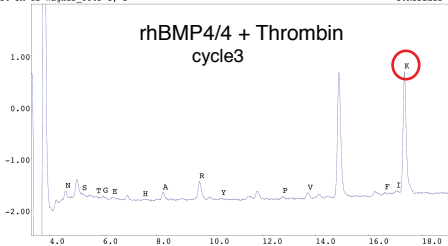
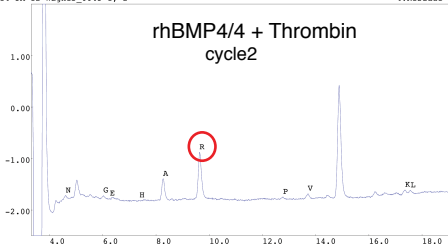
3:Residue 1

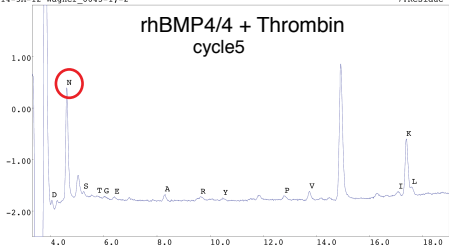
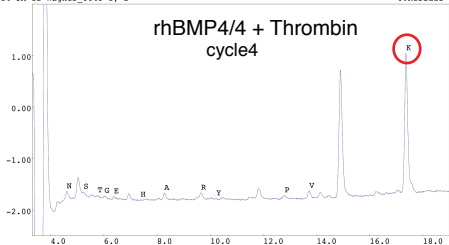


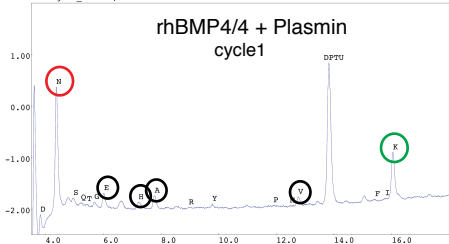
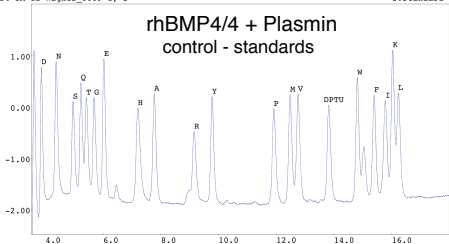






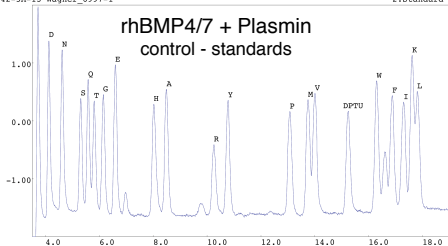






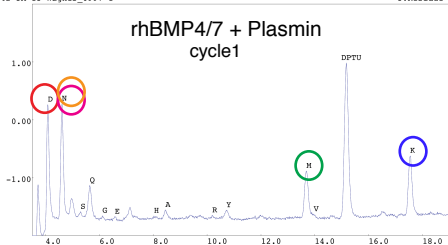
242-5A-13 Wagner_6997-1

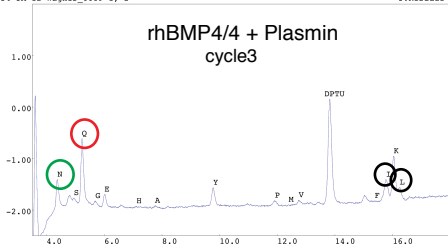
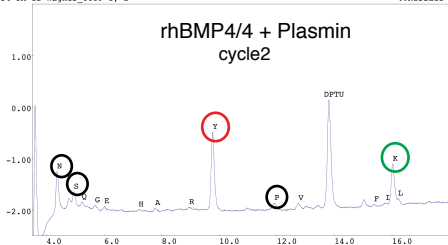
2:Standard 1

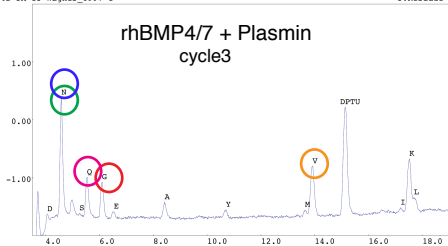
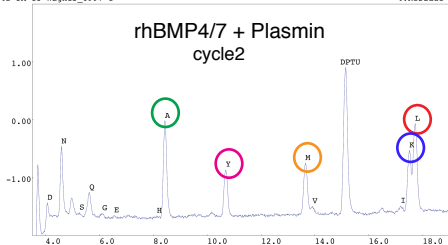


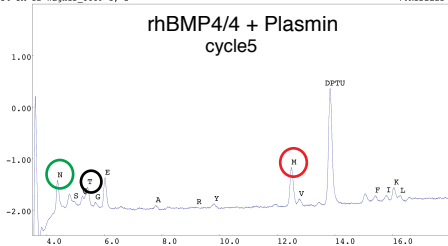
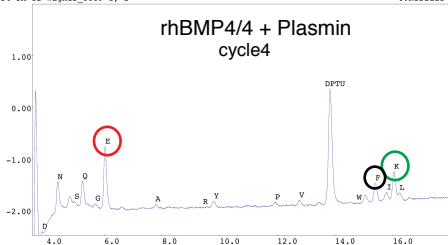
242-5A-13 Wagner_6997-1

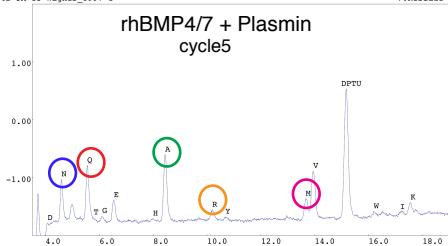
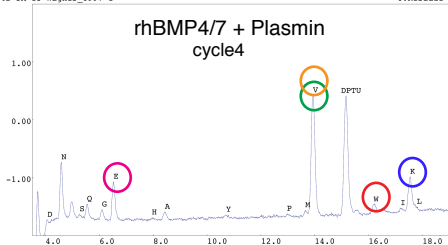
3:Residue 1











Data S1. Traces of Edman sequencing of rhBMPs. Relates to Figure 2, Figure S3 and TableS2.

Edman traces of rhBMP4/4 untreated/+plasmin/+thrombin as well as rhBMP4/7 + Plasmin are shown for individual Edman cycles (1-5). Colored circles (red, green, orange, blue, pink) highlight major amino acid peaks identified for each individual cycle. The corresponding colored circles in successive traces delineate a peptide that matches a BMP peptide sequence. Black circles highlight minor abundance amino acids that could not be assigned to the BMP query sequence and are most likely contamination.